

## Determining the Mode of Action of Ibomycin: A Novel Antifungal Compound

Determining the Mode of Action of Ibomycin: A Novel Antifungal Compound

By

DHRUV J. PATEL B.Sc

A Thesis Submitted to the School of Graduate Studies

In Partial Fulfillment of the Requirements for the

Degree of Master of Science

McMaster University

©Copyright by Dhruv J. Patel, August 2014

Descriptive Note

MASTER OF SCIENCE (2014)  
(Biochemistry and Biomedical Sciences)

McMaster University  
Hamilton, Ontario

Title: Determining the Mode of Action of Ibomycin: A Novel  
Antifungal Compound  
Author: Dhruv J. Patel, B.Sc (McMaster University)  
Supervisor: Dr. Gerard D. Wright  
Number of Pages: vii, 68

## **Abstract**

Unlike their bacterial counterparts, diseases caused by fungal pathogens are harder to treat due to a lack of discrete targets. Current antifungals are very broad spectrum and fall into three major classes: polyenes which target the cell membrane, azoles which target sterol biosynthesis and the echinocandins which target the cell wall. Recently a novel macrolide antibiotic produced by WAC 2288 was discovered in a co-culturing screen between various actinomycetes and pathogenic fungi. The active compound, a large type I polyketide compound called ibomycin, was specifically able to inhibit the growth of *Cryptococcus neoformans* but not *Candida albicans*. A combination of traditional and genetic approaches were used to identify the mode of action of ibomycin. Despite having characteristics associated with membrane perturbing agents such as fungicidal activity, causing hemolysis and even membrane localization *in vivo*, it does not seem that ibomycin disrupts the membrane in a sterol-dependent manner. We found evidence to suggest that ibomycin is not involved in disruption of cell wall biosynthesis based on localization *in vivo* and absence of viability rescue in presence of sorbitol. The results of haploinsufficiency and homozygous profiling of yeast deletion strains suggest that is no single protein target for ibomycin, but rather that membrane perturbation of ibomycin leads to downstream effects that impair vesicular trafficking and protein transport. Based on preliminary evidence, it is predicted that *C. albicans* is able to bind ibomycin but evades the induced toxic effects by barring access to its cell membrane.

## **Acknowledgements**

I would like to thank my parents, grandparents and my brother for always being there for me and being supportive in my quest to pursue science. I dedicate this thesis to you.

I would like to thank my supervisor Dr. Gerry Wright, for all of his guidance and support. Thank you for giving me this once in a lifetime opportunity to work with you and the other brilliant scientists part of the Wright lab. I am fortunate to have been part of a group that is constantly having a tremendous impact on the scientific community and am glad to be a member of the Wright lab legacy that will undoubtedly shine for years to come.

A great thanks to my committee members Dr. Marie Elliot and Dr. Michael Surette for all of their helpful discussions and comments. Thank you for bringing a fresh perspective to this work.

Thanks to all Wright Lab members, past and present for their support and for being fantastic mentors. It has been a pleasure to be amongst a group with such diverse expertise in various scientific fields. I can now boast that I have worked with the best!

A special thanks to my former TA, Jonathan O'Brien, for getting me started in the field antimicrobial drug discovery. Sure enough, I got to carry on where you had left off, and I thank you for laying the groundwork for the early stages of this project.

Thank you to Dr. Wenliang Wang for teaching me the ways of a natural product chemist.

Thank you to Nicholas Waglechner for assistance in all things bioinformatic.

A big thank you to Dr. Michaela Spitzer, Dr. Nicole Robbins and Laura Rossi for being my greatest resources of knowledge about fungi. Your expertise was an invaluable component of this project.

A special thank you to Peter Spanogiannopoulos, Andrew King, Dr. Grace Yim, Dr. Nicole Gilberger and Dr. Maulik Thaker for all of the helpful advice you've provided throughout my time in the lab. You have been great friends and mentors!

## Table of Contents

Abstract.....	iii
Acknowledgements.....	iv
List of Abbreviations.....	vii
Chapter 1: Introduction.....	1
1.1 Fungal pathogens in the clinic.....	1
1.1.1 <i>Cryptococcus neoformans</i> .....	1
1.1.2 <i>Candida albicans</i> .....	3
1.2 Current antifungal therapies.....	5
1.2.1 Azoles.....	5
1.2.2 Polyenes.....	7
1.2.3 Echinocandins.....	8
1.3 Sources of novel antifungals.....	9
1.4 Discovery of ibomycin.....	11
1.5 Biosynthesis of ibomycin.....	14
1.5.1 Polyketide biosynthesis.....	15
1.5.2 Sugar biosynthesis.....	18
1.6 Project Goals: Mode of action studies.....	19
Chapter 2: Materials and Methods.....	23
2.1 Ibomycin purification.....	23
2.2 Minimal Inhibitory Concentration (MIC) determination.....	24
2.3 Fungicidal activity assay.....	24
2.4 Hemolysis assay.....	25
2.5 Synthesis and purification of the ibomycin-bodipy conjugate.....	25
2.6 Fluorescent microscopy.....	26
2.7 Flow cytometry.....	27
2.8 Cell wall damage assay.....	28
2.9 Ergosterol feeding experiment.....	28
2.10 Chemical genetic screen.....	28
Chapter 3: Results.....	30
3.1 Ibomycin exhibits fungicidal activity.....	30
3.2 Ibomycin is hemolytic.....	30
3.3 Membrane localization of ibomycin-bodipy in <i>S. cerevisiae</i> .....	32
3.4 Flow cytometry.....	34
3.5 Ibomycin does not target the fungal cell wall.....	37
3.6 Ibomycin does not have an affinity for sterols.....	37
3.7 Yeast genome arrays.....	39
Chapter 4: Discussion.....	42
Future directions.....	46
Conclusion.....	47
References:.....	49
Appendix.....	55

## List of Figures

### Chapter 1

Figure 1.1: Chemical structures of various antifungal compounds.....	6
Figure 1.2: Discovery of ibomycin. ....	12
Figure 1.3: Ibomycin biosynthetic cluster.....	15
Figure 1.4: Proposed biosynthesis pathways for L-vancosamine, L-rhamnose and L-rhodinose from glucose-1-phosphate in WAC 2288. ....	20

### Chapter 3

Figure 3.1: Fungicidal activity of ibomycin.....	30
Figure 3.2: Hemolytic activity of ibomycin. ....	31
Figure 3.3: Ibomycin-bodipy synthesis reaction.....	32
Figure 3.4: Ibomycin localizes at the cell membrane. ....	33
Figure 3.5: Variable ibomycin-bodipy staining patterns in <i>C. neoformans</i> and <i>C. albicans</i> . ....	34
Figure 3.6: <i>C. albicans</i> cells stained with ibomycin-bodipy may not have compromised membranes. ....	36
Figure 3.7: Ibomycin does not have affinity for sterols. ....	38
Figure 3.8: Log <sub>2</sub> sensitivity scores of heterozygous deletion mutants to 10 µg/mL ibomycin. ....	40
Figure 3.9: Log <sub>2</sub> sensitivity scores of haploid deletion mutants to 8 µg/mL ibomycin. ....	41

### Supplementary

Supplementary Figure 1: Model for ibomycin biosynthesis. ....	56
Supplementary Figure 2: Sequence alignment of AT domains.....	58
Supplementary Figure 3: Vancosamine biosynthesis genes. ....	59
Supplementary Figure 4: Rhamnose biosynthesis genes. ....	60
Supplementary Figure 5: Differential staining between bodipy and ibomycin-bodipy. ....	62
Supplementary Figure 6: Unstained control samples of <i>C. neoformans</i> and <i>C. albicans</i> .....	63
Supplementary Figure 7: Growth curves of heterozygous deletion pool mutants in presence of ibomycin. ....	64
Supplementary Figure 8: Growth curves of haploid deletion pool mutants in presence of ibomycin. ....	65

## List of Tables

### Chapter 1

Table 1.1: Antifungal activity of ibomycin.....	14
---	----

### Chapter 3

Table 3.1- MICs of ibomycin-bodipy .....	33
Table 3.2-Ibomycin activity is undeterred in the presence of sorbitol.....	37

### Supplementary

Supplementary Table 1- Amino acid sequences of PKS docking domains .....	57
Supplementary Table 2-Primer sequences for amplification of upstream bar-coded tags from <i>S. cerevisiae</i> deletion strains .....	61
Supplementary Table 3- P-values for HIP hits grouped by GO processes .....	66
Supplementary Table 4- P-values for HOP hits grouped by GO Processes.....	67

## **List of Abbreviations**

ABC-Adenosine Triphosphate-Binding Cassette  
ACP-Acyl Carrier Protein  
AIDS-Acquired Immunodeficiency Syndrome  
AT-Acyltransferase  
ATCC-American Type Culture Collection  
BBB-Blood Brain Barrier  
BSA-Bovine Serum Albumin  
CLSI-Clinical and Laboratory Standards Institute  
DH-Dehydratase  
DMSO-Dimethyl Sulfoxide  
DNA-Deoxyribonucleic Acid  
EDTA-Ethylenediaminetetraacetic Acid  
ER-Enoyl Reductase  
GO-Gene Ontology  
GPI-glycosylphosphatidylinositol  
GXM-Glucuronoxylomannan  
HAART-Highly Active Antiretroviral Therapy  
HIP-Haploinsufficiency Profiling  
HIV-Human Immunodeficiency Virus  
HOP-Homozygous Profiling  
HPLC-High Performance Liquid Chromatography  
KR- $\beta$ -Ketoreductase  
KS-  $\beta$ -Ketosynthase  
MFS-Major Facilitator Superfamily  
MIC-Minimal Inhibitory Concentration  
NMR-Nuclear Magnetic Resonance  
NRPS-Non-ribosomal Peptide Synthase  
PBS-Phosphate Buffered Saline  
PKS-Polyketide Synthase  
RBC-Red Blood Cell  
RNA-Ribonucleic Acid  
RPMI-Roswell Park Memorial Institute medium  
UV-Ultraviolet  
WAC-Wright Actinomycete Collection  
YNB-Yeast Nitrogen Base medium  
YPD-Yeast extract Peptone Dextrose medium

## **Chapter 1: Introduction**

### **1.1 Fungal pathogens in the clinic**

The Fungal kingdom encompasses a wide variety of unicellular and multicellular organisms that are capable of inhabiting diverse niches. While many fungal species pose no major threat to humans, a small handful of species are classified as opportunistic pathogens and pose major threats to human health. Within the last two decades, incidences of fungal infections have become increasingly prevalent in the clinic (1). Certain ailments such as athlete's foot, caused by *Trichophyton rubrum*, can be treated with relative ease. However, certain fungal infections are systemic and their effects go largely unnoticed until individuals become immunocompromised. With the onset of HIV/AIDS cases across the globe and the increased use of immunosuppressant drugs for cancer treatments and organ transplants, a greater percentage of the population is now immunocompromised and thus more susceptible to acquiring fungal infections. In particular, fungal infections caused by *Cryptococcus neoformans* and *Candida albicans* are the most prominent and are associated with high mortality rates (2).

#### *1.1.1 Cryptococcus neoformans*

The basidiomycete *Cryptococcus neoformans* was discovered nearly 120 years ago concurrently by Busse in Germany and Sanfelice in Italy. Both discoveries led to very crucial information regarding the organism. Busse, a pathologist, identified the microorganism from a lesion in a patient's leg (3), while Sanfelice had originally isolated the organism from fermented peach juice before establishing its pathogenicity through

animal studies (4). These findings revealed that the fungus was not exclusively found in nature but that it was also associated with disease in humans. It wasn't until the early 1980s that this fact became apparent again with the onset of HIV/AIDS. Prior to then, fungal related illnesses were quite rare and common only to tropical and sub-tropical regions with the causative agents being non-*Cryptococcus* species (5). When the AIDS epidemic began in 1981, there was a concurrent rise in the number of *C. neoformans* infections. Even today, regions that don't have access to Highly Active Antiretroviral Therapy (HAART), for example Sub-Saharan Africa, showcase surprisingly high incidences of cryptococcosis and equally high mortality rates (6).

*C. neoformans* primarily causes subcutaneous infections that originate in the lungs and then subsequently spread to other areas of the body. Infection begins with the inhalation of spores from the environment, which can be found in pigeon guano as well as the bark and leaves of trees and decaying plant material (7). The basidiospores remain in a dormant state in the alveoli of the human host, primarily through the phagocytic activity of macrophages (8). In the event that the body becomes immunocompromised, the basidiospores germinate using the macrophage as a vehicle to cross the blood brain barrier (BBB). Studies have shown that this step is vital for successful dissemination into the brain, as depletion of macrophages leads to a lack of colonization in the brain and delayed death phenotype in mice (9). Once the BBB has been penetrated, the yeast can colonize within the meninges. This eventually leads to inflammation of the meninges, a condition known as meningitis or meningoencephalitis.

The two major features that make *C. neoformans* a particularly dangerous and effective pathogen are its thick polysaccharide capsule and the presence of melanin in the cell wall. The polysaccharide capsule is composed mainly of glucuronoxylomannan (GXM) and galactoxylomannan as well as small amounts of mannoproteins (10). This feature of *C. neoformans* is critical in escaping detection by host defense mechanisms. Firstly, the large capsule prevents efficient phagocytosis of the pathogen by white blood cells, thereby allowing it to remain in the pulmonary system. Furthermore, it has been shown that even if the pathogen is engulfed by the leukocytes, it quickly disables production of pro-inflammatory signals by releasing GXM into the cytoplasm (11). The presence of melanin in the cell wall is also a vital means of survival for *C. neoformans* in the host. Melanin has been shown to help the pathogen deal with the high levels of reactive oxygen species produced by the host's immune system (12).

### 1.1.2 *Candida albicans*

The ascomycete *Candida albicans* has long been renowned as the most prevalent fungal pathogen. Hippocrates first described an ailment he had observed as “aphthae in the mouth” (13), a condition known today as oral thrush – a result of *C. albicans* colonization of the mouth. Throughout the 19<sup>th</sup> century, several physicians and mycologists isolated *C. albicans* in its yeast and filamentous forms from patient samples (14). Today, *C. albicans* is considered a commensal organism and component of the human microbiota, but is also shown to be implicated in various cutaneous and systemic infections, collectively known as candidiasis. Normally, superficial levels of fungal

growth are controlled by the natural microbiota and the skin remains an adamant barrier, preventing entry and dissemination inside the body. Ailments such as oral thrush or vulvovaginal candidiasis are examples of superficial overgrowth of the fungus and are considered non-lethal. Systemic infections caused by this opportunistic pathogen can be lethal and affect several organs including the lungs, gastrointestinal tract and brain.

There are several virulence factors attributed to *C. albicans* that are important for pathogenicity, the three most important being adhesion to biotic and abiotic surfaces, dimorphism between yeast and hyphal stages and secretion of hydrolytic enzymes. Dissemination of *C. albicans* begins with adherence of yeast cells to either host cells or abiotic surfaces using several adhesins that are linked to the membrane via glycosylphosphatidylinositol (GPI) anchors. Adhesion of yeast cells to host cells can trigger one of two processes: induced endocytosis or active penetration (15). This is a fundamental step in the establishment of the pathogen and not surprisingly mutants lacking various adhesins show attenuated virulence (16). Adherence to abiotic surfaces such as catheters often leads to the formation of biofilms, which can easily introduce the organism into the systemic circulation and subsequently adhere to body tissues. This is evident from the fact that *C. albicans* is now the fourth leading cause of hospital-acquired bloodstream infections (17). Once the organism has attached to the host cells it is able to transition from its unicellular yeast stage into a filamentous hyphal form, a required feature for invasive tissue damage. The switch to hyphal form is triggered by a variety of environmental cues including pH, temperature, carbon dioxide (CO<sub>2</sub>) levels and presence

of N-acetylglucosamine (18). In this form, the organism is also able to actively produce and secrete proteases, lipases and phospholipases which it uses to obtain nutrients from its environment and break down host tissue for further colonization.

## 1.2 Current antifungal therapies

Fungi are eukaryotic organisms and therefore pose a major hurdle when searching for drug candidates with minimal host toxicity. Unlike bacterial pathogens, there are few fungal specific targets that are not shared with mammalian cells. A majority of the antifungals available for clinical use fall into three classes: the azoles, the polyenes and the echinocandins (Figure 1.1). Structurally, they are all distinct and target various aspects of fungal biology.

### 1.2.1 Azoles

Azoles encompass a large class of synthetic compounds that inhibit production of ergosterol. The two major types of azoles currently in clinical use are either imidazole-based or triazole-based (19, 20). These compounds bind and inhibit C14 $\alpha$ -demethylase, an enzyme involved in the production of ergosterol. C14 $\alpha$ -demethylase is encoded by the gene *ERG11* and catalyzes the demethylation of lanosterol, an early intermediate in ergosterol biosynthesis, to produce 4,4-dimethylcholesta-8,14,24-trienol. Inhibition of C14 $\alpha$ -demethylase activity not only leads to an overall decrease in ergosterol production (hence affecting membrane fluidity) but also leads to the accumulation of toxic intermediates which induce membrane stress responses (21). These combined outcomes

lead to an inhibition of growth of the fungal pathogen, and as a result the azoles are defined as fungistatic agents.

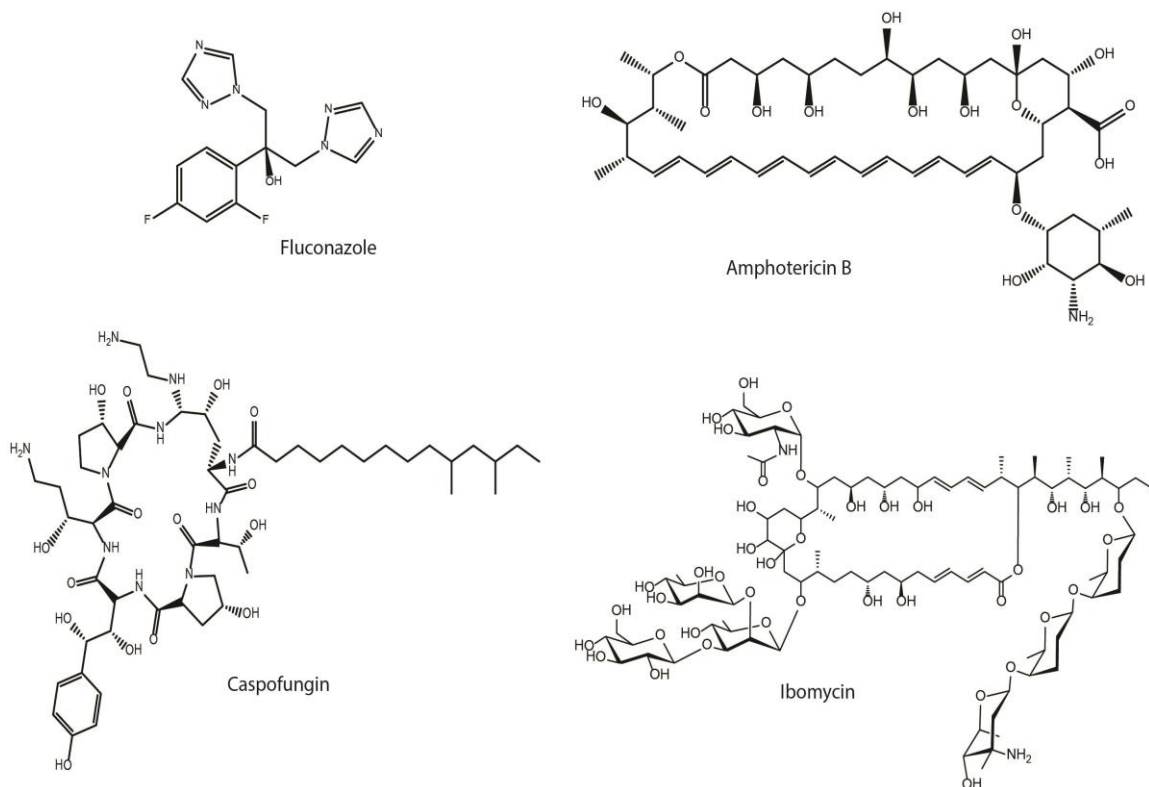


**Figure 1.1: Chemical structures of various antifungal compounds.** Fluconazole is a triazole and targets ergosterol biosynthesis. Amphotericin B is a large, amphipathic polyene involved in membrane disruption. Caspofungin is a lipopeptide echinocandin that targets cell wall biosynthesis. Ibotomycin is a novel type I polyketide antifungal that has specific anticryptococcal activity and is believed to be involved in membrane disruption in a manner independent of the polyenes.

Resistance to azoles is quite common after periods of prolonged use and can occur through a variety of mechanisms. The most common mechanism is through increased expression of multidrug efflux proteins such as *AFRI* in *C. neoformans* (22). In *C. albicans*, transcriptional regulators such as *Tac1* and *Mrr1*, which control expression of ATP-Binding Cassette (ABC) transporters (23) and Major Facilitator Superfamily (MFS)

transporters (24) respectively, are up-regulated to ensure efficient removal of the azoles from the cell. Alternatively, resistance can also be achieved through mutational alteration of the Erg11 protein. These amino acid substitutions decrease the affinity of Erg11 for azoles without affecting the binding affinity for the native substrate. Several unique amino acid substitutions have been reported in the *ERG11* gene in *C. albicans* (25). It has also been shown that different combinations of mutations can confer varying levels of resistance to a variety of azoles (26, 27).

### 1.2.2 Polyenes

The polyenes are large amphipathic molecules with several double bonds. They are a common antifungal agent produced and secreted by soil actinomycetes (28). It is widely accepted that polyenes such as amphotericin B bind to ergosterol in fungal membranes leading to the formation of functional pores, which allow for the release of ions from fungal cells and ultimately leading to cell death. This mode of action is highly plausible based on the structure of polyenes. A series of double bonds result in the formation of a long planar conjugated system which can interact with the planar ring system of sterols (29). In addition, the sugar moiety along with the carboxylic acid substituent of the hemiketal ring forms a polar head which interacts with the 3 $\beta$ -OH of sterols. Together these interactions allow for the formation of a tight polyene-sterol complex. A collection of these complexes can then be arranged to form a transmembrane pore structure that would facilitate leakage of ions from the cell (30).

Although resistance to polyenes is quite rare, the major issue with the use of polyenes as antifungals is host toxicity. Studies have shown that polyenes can bind to the cholesterol found in mammalian cell membranes (29). In fact, several polyenes have been shown to have a hemolytic effect on erythrocytes (31). Efforts have been made to generate analogs that are less toxic to the host yet retain antifungal activity (32).

### 1.2.3 Echinocandins

The cell wall is an extracellular feature that is present in fungi, plant cells and bacteria. Fungal cell wall composition also varies between species. Major constituents include several polysaccharides such as chitin and glucans and glycoproteins usually tethered by GPI-anchors (33). *C. neoformans* also has a capsule made of complex mannose polymers and mannoproteins (10). The major function of the cell wall is to provide osmotic stabilization. Fks1, a (1,3)- $\beta$ -D glucan synthase, is a major cell wall associated protein involved in production of the glucan layer. It is the target of the most recent class of antifungals, the echinocandins. Through inhibition of cell wall biosynthesis, echinocandins such as caspofungin initiate cell wall stress responses. Fungal cells are unable to cope with changes in osmotic pressure and eventually die.

Echinocandins were originally isolated as pneumocandins which are cyclic lipopeptides made using non-canonical amino acids and produced by the filamentous fungus *Glarea lozoyensis* (34). However these compounds were found to be quite toxic for mammalian cells and displayed a limited antifungal spectrum and thus did not

proceed far in clinical trials. Semisynthetic analogs with lower toxicity were eventually developed and gave rise to the first novel class of antifungals available in the clinic within the past 20 years. The three commercially available echinocandins in use today include caspofungin, micafungin and anidulafungin which are active against *C. albicans* and *A. fumigatus* (34, 35). Surprisingly despite having a functional Fks1 protein, echinocandins remain ineffective against *C. neoformans*. *In vitro* studies have shown that Fks1 isolated from *C. neoformans* is sensitive to echinocandins, but they are not active *in vivo* (36). This suggests that *C. neoformans* is intrinsically resistant to this class of antifungals and may be evading their inhibitory effects by other means such as efflux or degradation. Similar to azole resistance, *C. albicans* resistance to echinocandins usually arises through mutations in the target (37), Fks1, or less commonly through increased efflux of the drug (35).

### 1.3 Sources of novel antifungals

As with antibacterial compounds, fungal pathogens can readily develop resistance to antifungal agents. Resistance to the azoles and amphotericin B have already been reported in the clinic (38). Several other compounds, both natural products and synthetics, are being probed for antifungal activity to meet the demands of the clinic (39). In particular, compounds with alternative mode of actions are interesting.

Actinomycetes are leaders in secondary metabolite production. They are known producers of several classes of antimicrobial and anticancer compounds (40). The chemical diversity of secondary metabolites produced and secreted by actinomycetes can

be attributed to the highly competitive environments that they reside in. They can be found in a wide variety of niches from common soil samples to salt pans, cold and hot deserts and marine environments (41-44). In these regions, resources are scarce either due to limited availability and strict competition with other organisms. For example, most soil actinomycetes live in a biologically diverse setting, where they must compete for resources with other bacterial species and fungi (45). Hence it seems logical that actinomycetes would produce bioactive compounds that antagonize the growth of these competitors, and subsequently bolster their survival. Fortunately, we have been able to harvest this chemical potential, which has evolved over millennia (40), to combat infectious diseases caused by bacteria, fungi and viruses. However there are likely thousands of compounds that have not yet been discovered or isolated from actinomycete species (46, 47). This may be due to the fact that we are still largely unaware of the specific conditions that prompt secondary metabolite production in actinomycetes. Identification and analysis of biosynthetic clusters as well as their regulatory elements may be the key to finding novel chemical diversity. The activation of cryptic clusters through various methods has already been used to isolate several novel natural products (48, 49).

The Wright Lab has developed a novel phenotypic screen in attempts to discover uncharacterized chemical diversity from particular types of actinomycete strains known as endophytic actinomycetes. These bacteria are found in or on various plant structures including the roots, leaves, stems and inner tissues (50) and typically share an

endosymbiotic relationship with their host (51). The plant provides a habitable environment and sufficient nutrients for the endophyte which in return secretes a variety of antimicrobial compounds that provide protection against plant-pathogenic fungi (52). Thus endophytic actinomycetes appear to be a relatively untapped resource of antifungal compounds.

#### **1.4 Discovery of ibomycin**

The development of a novel co-culturing screen was the first step in the discovery of ibomycin. Previous work by other groups had shown that co-cultivating bacteria and fungi serves as an effective means to induce secondary metabolite production from both microorganisms (53-55). This may be due to the fact these methods stimulate microbial interactions that actually occur in the environment. The Wright lab has added a unique twist to this approach by co-culturing endophytic actinomycetes in close proximity to two pathogenic fungal species, *C. neoformans* and *C. albicans* on solid agar (56). This is the first reported use of either of these pathogens in this type of study.

The initial aim of this experiment was to observe any induced phenotypic changes in either the bacteria or fungi as a result of the co-culturing and subsequently identify the metabolites responsible for these changes. Certain strains of actinomycetes began secreting coloured metabolites, while others secreted agents that induced hyphal growth of *C. albicans*. Strains which produced polyenes or broad-spectrum antifungals were easily identified as they eliminated growth of both pathogenic fungi.

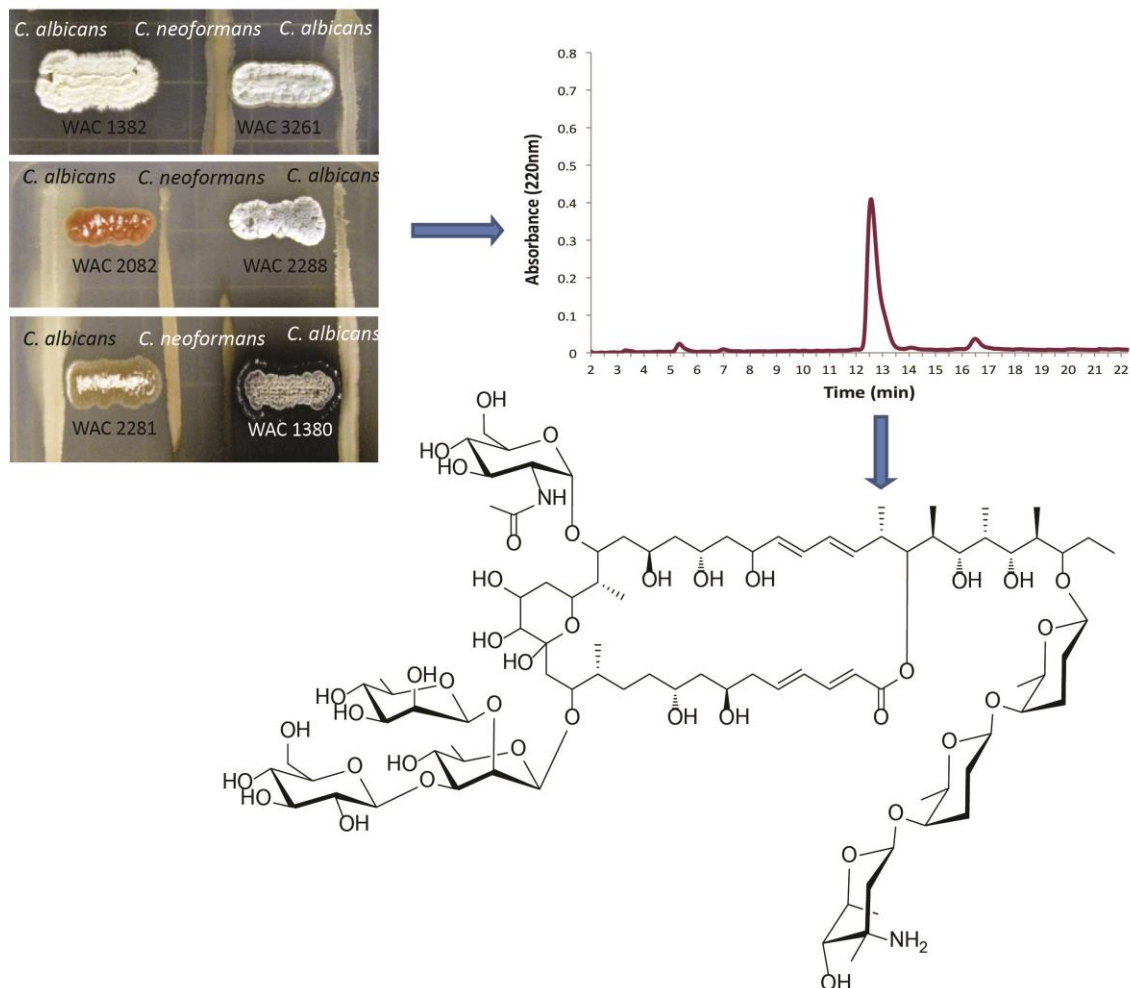


**Figure 1.2: Discovery of ibomycin.** Ibomycin was discovered in a co-culturing screen using endophytic actinomycetes and the pathogenic fungi *C. neoformans* and *C. albicans*. The strain WAC 2288 displayed an interesting phenotype as it was able to inhibit the growth of *C. neoformans* but not *C. albicans*. Subsequent large scale culturing of WAC 2288 led to the purification of a single peak which re-capitulated the results of the co-culturing screen. Structural analysis of the purified compound showed it to be a novel large type I polyketide compound called ibomycin.

An interesting result was obtained using a *Streptomyces sp.*, WAC 2288 which selectively inhibited growth of *C. neoformans* but did not affect *C. albicans* (Figure 1.2). Large scale culturing of WAC 2288 led to the purification of a type I polyketide compound called ibomycin, which recapitulated the results from the co-culturing

experiments. The structure of ibomycin was elucidated based on results from several 1D and 2D NMR experiments and mass spectrometry analysis. Aside from its interesting bioactivity, other noticeable features of the molecule include its vast size (molecular weight: 1932 g/mol) and the presence of a seven sugars on the macrolactone scaffold (Figure 1.2). Further tests also showed that ibomycin was biologically active against other cryptococcal species such as *Cryptococcus gattii*, as well as the model yeast organism *Saccharomyces cerevisiae*. Interestingly, all species of *Candida* tested were resistant to ibomycin (Table 1.1).

**Table 1.1: Antifungal activity of ibomycin.**

<b>Organism</b>	<b>MIC (<math>\mu\text{g/mL}</math>)</b>
<b><i>Cryptococcus neoformans</i> H99</b>	<b>4</b>
<b><i>Cryptococcus gatti</i>-Clinical isolate</b>	<b>4</b>
<b><i>Saccharomyces cerevisiae</i> BY4741</b>	<b>8-16</b>
<i>Candida albicans</i> (ATCC 92114)	64
<i>C. albicans</i> Amphotericin B Resistant isolate	64
<i>C. albicans</i> Fluconazole Resistant-clinical isolate 1	>128
<i>C. albicans</i> Fluconazole Resistant-clinical isolate 2	64
<i>Candida glabrata</i> -Clinical isolate	128
<i>Candida tropicalis</i> (ATCC 20956)	64
<i>Candida parapsilosis</i> (ATCC 90018)	64

## 1.5 Biosynthesis of ibomycin

In order to understand how a molecule as large as ibomycin was being synthesized, the genome of WAC 2288 was sequenced and subsequently scanned for a putative biosynthetic cluster. A draft genome was prepared using a combination of sequencing data from 454 pyrosequencing and mate-paired end Illumina sequencing and assembled on 237 contigs (N50 = 138,212) using MIRA. The 8.6 Mb genome was scanned for putative type I polyketide biosynthetic clusters using AntiSMASH, an online program specializing in the prediction of secondary metabolite clusters (57). A candidate 140 kb cluster was found, encompassing 40 genes, 7 of which are type I polyketide synthase (PKS) genes, comprising 69 kb of the cluster (Figure 1.3). The remainder of the

cluster contains genes involved in regulation, sugar biosynthesis, efflux and various tailoring enzymes.

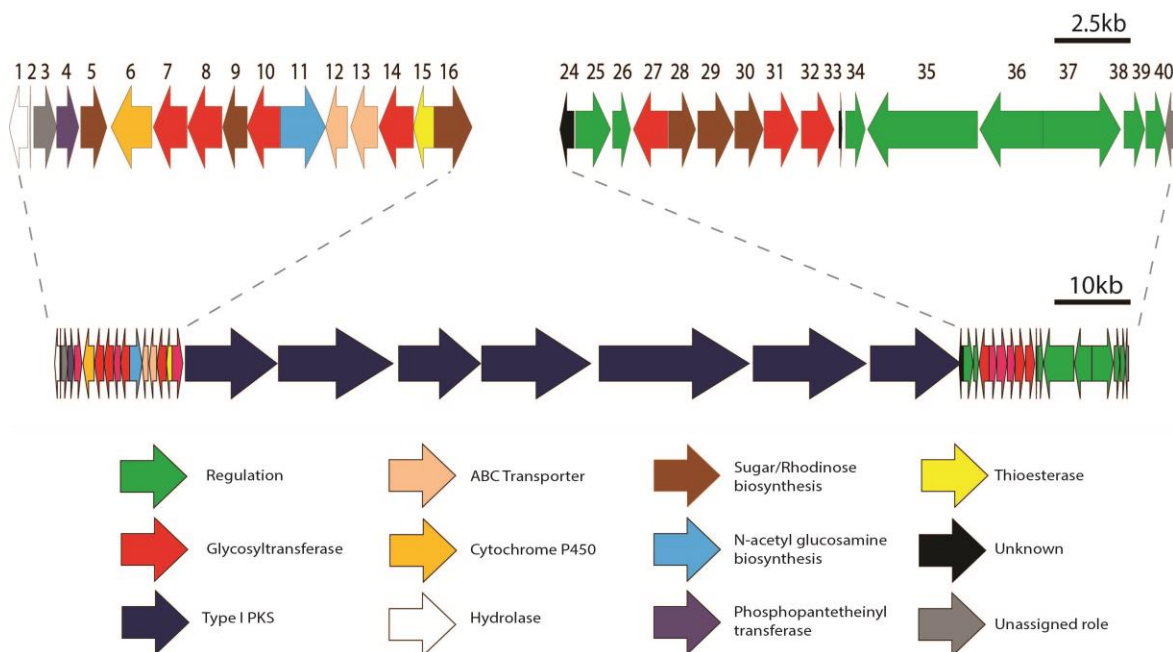


**Figure 1.3: Ibomycin biosynthetic cluster.** A 140 kb cluster predicted to synthesize a type I PKS was found in the genome of WAC 2288 using antiSMASH. The cluster is composed of 40 genes, 7 of which are responsible for production of the PKS scaffold. The remaining genes are involved in regulation, efflux, sugar biosynthesis and decoration of the scaffold.

### 1.5.1 Polyketide biosynthesis

The large macrolactone backbone of ibomycin is synthesized in its entirety using PKS bio-machinery. These multi-enzyme complexes are largely similar to those used for fatty acid biosynthesis in prokaryotes and eukaryotes (58). However, while traditional fatty acid synthesis is accomplished through re-iterative addition of malonyl-CoA subunits which are all reduced to produce a saturated hydrocarbon, polyketides can be synthesized using a variety of acyl subunits and there are usually variable degrees of

unsaturation throughout the chain. Polyketide biosynthesis also occurs in a modular fashion with each module catalyzing the addition of a single acyl subunit and subsequently reducing the  $\beta$ -keto ester as necessary. The simplest of modules contains 3 domains: an acyltransferase (AT) domain, a ketosynthase (KS) domain and an acyl carrier protein (ACP) domain. The AT and KS domains are responsible for selecting and condensing monomer subunits respectively while the ACP domain serves as a scaffold for the growing polyketide chain. The most common monomers for polyketide biosynthesis are malonyl-CoA and methylmalonyl-CoA and their specificity of use during synthesis is determined by signature amino acids in the AT domains (59).

Modules can also include a combination of ketoreductases (KR), dehydratases (DH) or enoyl reductases (ER) to reduce the  $\beta$ -keto ester and generate various functional groups (60). For example, the presence of a KR domain will produce a hydroxyl moiety by reducing the  $\beta$ -keto group. The combination of KR and DH domains will cause further reduction of the hydroxyl moiety to an alkene group. It should be noted that the absolute stereochemistry of the  $\beta$ -hydroxyl and alkene groups are dictated by specific amino acid residues in the catalytic sites of the KR and DH domains respectively (61, 62). The presence of an ER domain in combination with KR+DH will produce a fully reduced methylene unit.

In the case of ibomycin, there are 7 PKS genes encoding a total of 86 catalytic domains that form the 20 modules responsible for the production of a 41 carbon backbone. All enzymes are predicted to be functional except a DH domain in module 12.

The order of the modules is also quite accurate with the structure elucidated by NMR data, however there are a couple of notable differences. Based on the elucidated structure a more likely model of ibomycin biosynthesis would have the domains of modules 12 and 13 switched with each other as well as those in modules 14 and 15, as shown in Supplementary Figure 1. Typically the order of PKS genes for assembly of the polyketide is determined by matching docking domains. Each multi-domain protein is flanked by N- and C-terminal docking domains at either ends for docking of the correct protein in the assembly line, ensuring faithful progression of the maturing polyketide chain. Docking domains were identified in the translated sequences of all the PKS genes except *ibo18* and *ibo21* which lacked a C-terminal docking domain and *ibo20*, which lacked both docking domains (Supplementary table 1). The absence of these domains suggests that they may have non-canonical docking pairs and thus have escaped detection by the existing software, which have been designed based on known docking domain sequences (63). Sequence analysis of the 20 AT domains indicated 11 malonyl-CoA and 9 methyl malonyl-CoA as the substrates that make up the polyketide chains (Supplementary Figure 2). All but 4 of these AT domains predict the correct monomer as seen in the structure of ibomycin. It is unclear whether these types of discrepancies are quite common, however a few cases have been reported in the literature (64, 65).

The NMR data suggests the presence of a hydroxyl moiety on C16, which is presumed to be added as post-PKS modification by *ibo6*, a cytochrome P450 monooxygenase in the cluster. This event could be indirectly triggering macrocyclization

by spatially orienting the C15 carbonyl group towards C19 hydroxyl group to form an internal hemiketal ring. This feature would then lock the molecule in a conformation that brings the C1 carbonyl group in close proximity to the hydroxyl moiety of C37. This also explains specificity and choice of hydroxyl carbon for macrocyclization from a series of options present on the polyketide tail.

### 1.5.2 Sugar biosynthesis

With such a multitude of sugars decorating the polyketide structure of ibomycin, it is interesting to examine how they are all synthesized. Depending on the complexity, sugars attached to natural products may be obtained from metabolites in the environment or synthesized *de novo* starting with glucose-1-phosphate as a substrate. Surrounding the PKS genes are a number of potential tailoring enzymes such as glycosyltransferases and a cytochrome P450 oxidase, which are believed to be involved in modification of ibomycin after synthesis of the polyketide backbone. The biosynthesis of L-rhodinose is also proposed to occur using some of these genes. Their functions were predicted and annotated based on nucleotide sequence comparison of the genes in question with known rhodinose biosynthesis genes (66-68). Acquisition of N-acetylglucosamine is proposed to occur using the product of *ibo11*, a  $\beta$ -N-acetylhexosaminidase (Figure 1.3).

Based on previously identified clusters the WAC 2288 genome was scanned for vancosamine and rhamnose biosynthesis genes (69, 70). Genes for vancosamine biosynthesis, annotated as *ivaA-E*, were found on a separate contig distant from the ibomycin biosynthetic gene cluster. This was particularly interesting because in the case

of glycopeptide antibiotics (GPA) which contain vancosamine or its derivatives, the genes for vancosamine biosynthesis are typically located within the GPA biosynthesis cluster (71). Furthermore, the arrangement of the *iva* genes was highly unconventional with *ivaA* (a C2-dehydratase involved in the early stages of vancosamine biosynthesis) located approximately 74 kb downstream of the other genes (Supplementary Figure 3), embedded within an NRPS-PKS hybrid cluster (as predicted by AntiSMASH).

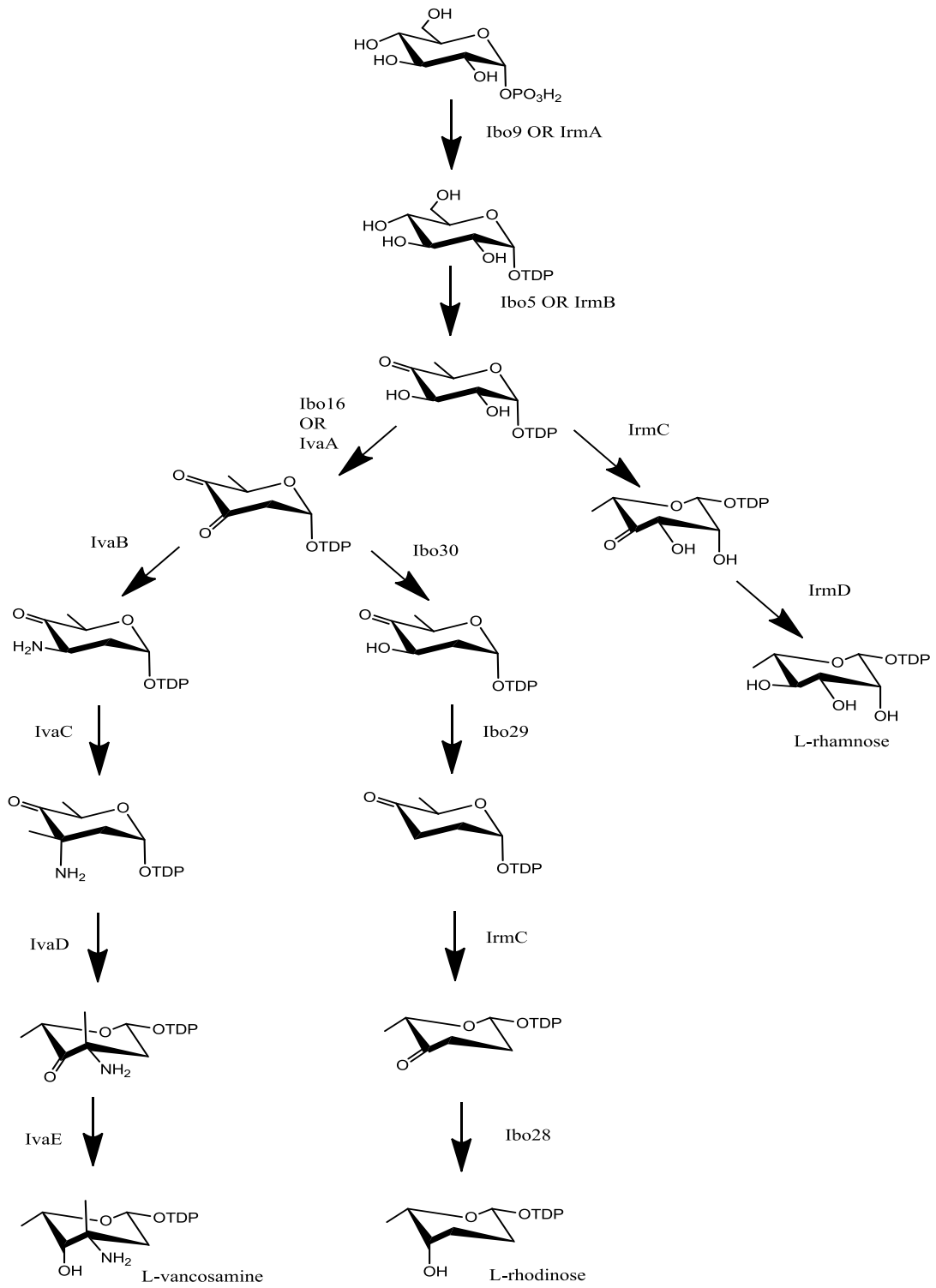
Similarly, the rhamnose biosynthesis genes, annotated as *irmA-D*, were found on a separate contig and located approximately 38 kb downstream of a cluster predicted to synthesize a terpene (Supplementary Figure 4). It is not yet known if the other biosynthetic clusters that are in proximity with the sugar biosynthesis genes are actively expressed or if their predicted metabolites are co-secreted with ibomycin. Nonetheless, this phenomenon of using sugar biosynthesis genes from other biosynthetic clusters does not appear to be a very common one. Interestingly, it appears that as three out of the five different sugars attached to the ibomycin aglycone are deoxy-L-sugars, they share some of their biosynthesis genes, particularly in the early stages. A proposed biosynthesis scheme for these sugars and possible enzymatic substitutions in each pathway is illustrated in (Figure 1.4).

## **1.6 Project Goals: Mode of action studies**

The unique bioactive profile of ibomycin warrants investigation into its mode of action. This information will not only help gauge its potential as an antifungal agent that can be used in the clinic, but may also provide insight on how resistant organisms such as

*C. albicans* are able to evade its effect. There are a variety of target identification methods that can be used to accomplish this task. Traditional approaches such as development of fluorescent analogs could be used to monitor localization of the compound *in vivo*. A bioactive analog of ibomycin lacking the vancosamine sugar has been isolated (56), suggesting that modifications at the free amine of vancosamine (e.g. addition of fluorescent probe) should not hinder the efficacy of the compound as an antifungal agent. Alternatively, experiments that have been used to deduce the mode of action for known antifungals could be attempted with ibomycin to determine if similar results are obtained. For example, previous studies of various polyenes have shown that they frequently cause hemolysis in erythrocytes and  $K^+$  leakage in fungal cells (31) and bind sterols with high affinity (29). Results from these kinds of assays with ibomycin would reveal the novelty of its mode of action.

**Figure 1.4: Proposed biosynthesis pathways for L-vancosamine, L-rhamnose and L-rhodinose from glucose-1-phosphate in WAC 2288.** L-vancosamine biosynthesis is proposed to occur using IvaA-E. L-rhamnose biosynthesis is proposed to occur using IrmA-D. L-rhodinose is proposed to be synthesized using various genes in the ibomycin cluster. Several enzymes in the early stages of each biosynthetic process appear to have close homology and may be substituted with each other (e.g. Ibo9/IrmA, Ibo5/IrmB, and Ibo16/IvaA).



Alternatively since ibomycin is active against *Saccharomyces cerevisiae*, the use of chemical genetic screens with yeast deletion collections may provide some assistance. Haploinsufficiency profiling (HIP) and homozygous profiling (HOP) using the *S. cerevisiae* yeast deletion collection (72, 73) would reveal deletion strains that are hypersensitive to ibomycin, thereby determining the genes and pathways that are important for fitness in the presence of ibomycin.

This work attempts to decipher the mode of action of ibomycin using all of the aforementioned approaches. Results suggest that ibomycin localizes at the membrane and is likely involved in membrane disruption but in a manner unlike that of the polyenes. The fungal cell wall does not appear to be a target, but rather it may act an intrinsic barrier that prevents activity against species of *Candida*. The results of the HIP/HOP assays suggest that there is no single protein target for ibomycin, but rather that it is exerting its effects on pathways related to cell organisation and biosynthesis.

## **Chapter 2: Materials and Methods**

### **2.1 Ibomycin purification**

WAC 2288 was fermented in six 1 L flasks of Bennett's medium for seven days at 30°C. The cell pellet was separated from the conditioned medium using a cellulose membrane (Whatman #4) for eventual solid and liquid extraction of the active compound. The conditioned medium was concentrated using rotary evaporation before being combined with 25 g of HP-20 resin (Sigma) and incubated overnight at 4°C with shaking. The resin-bound compound was subsequently packed into a chromatography column and washed with water and 80% methanol before elution with 100% methanol. C18 reversed phase flash chromatography (*CombiFlash*) using a 26 g RediSEP column (Teledyne ISCO, Inc. Lincoln, NE, USA) was used as a secondary purification step (mobile phases of water (A) and methanol (B), both containing 0.05% formic acid). The following gradient was used: 0 min 80% A/20% B, a linear gradient from 0 to 2 min up to 60% B and from 2 to 22 min up to 100% B, followed by 7 min of 100% B at a flow rate of 25 mL/min. A broad peak was detected from 18.5-25 min with absorbance at 220 and 226 nm. Fractions containing ibomycin were pooled, dried and re-suspended in methanol before purification by reversed phase HPLC (Waters e2695) using a C18 semi-preparative column (Waters XSelect CSH prep C18 5µm, 10x100mm). The mobile phases were water (A) and acetonitrile (B), both containing 0.05% formic acid. The method used was as follows: 0 to 1 min 32% B, a linear gradient from 1 to 13 min up to 36.5% B and from 13 to 14 min up to 100% B, followed by 100% B for 1.2 min, and then

a linear gradient for 1 min down to 32% B at a flow rate of 4 ml/min. Absorbance was measured at 220 and 266 nm and the compound eluted as a broad peak with a retention time of 9.6 min. In order to further extract the active compound, the cell pellet was mixed with 1 L of methanol overnight before filtering out the cellular debris. The methanol extract was subsequently dried and re-suspended in methanol and purified as described above.

## **2.2 Minimal Inhibitory Concentration (MIC) determination**

Yeast MICs were conducted using the standardized broth microdilution method, as per CLSI protocols (74). The assays were carried out in 96-well microtiter plates with a total volume of 0.2 mL/well with 2-fold dilutions of test compounds dissolved in DMSO. Strains were grown in Yeast Peptone Dextrose (YPD) medium overnight at 30°C unless otherwise stated. The inoculum was prepared by determining the density of an overnight culture and diluting such that approximately  $10^3$  cells were added to each well. Plates were incubated at 30°C for 48 hours before absorbance was measured at 600 nm.

## **2.3 Fungicidal activity assay**

An overnight culture of *C. neoformans* H99 in RPMI was diluted to an  $OD_{600}$  of 0.1 before being further diluted 1:1000 into 5 mL RPMI media. Cultures were treated with 0.1% DMSO (control) or 2 µg/mL, 4 µg/mL or 16 µg/mL ibomycin in DMSO and incubated at 37°C with shaking. At pre-determined time points (0, 6, 12, 24 and 48 hours) a 0.1 mL sample from each culture was diluted ten-fold six times before being streaked

onto Sabouraud-dextrose agar. Plates were incubated at 37°C and allowed to grow for at least 48 hours before performing colony counts. A similar assay was performed using *Staphylococcus aureus* CMRSA2 and 64 µg/mL ibomycin.

#### **2.4 Hemolysis assay**

A sample of heparinized human blood was centrifuged for 5 min at 3000 rpm. The supernatant containing the plasma and buffy coat was removed before washing the red blood cell (RBC) pellet twice with 0.85% saline with 5 mM EDTA. Washed RBCs were re-suspended in saline to prepare a 4% v/v solution. Serial dilutions of ibomycin, devancosamyl ibomycin and amphotericin B were prepared in DMSO and 2.5 µL of compound was added to 47.5 µL of saline and 50 µL of the RBC suspension in a 96-well plate. Triton X (0.1%) was used as a 100% lysis control and 2.5% DMSO as a negative control. The plate was incubated at 37°C for 2 hours. Following incubation the plate was centrifuged at 3000 rpm for 10 min and the supernatant was collected to measure the hemoglobin content at 541 nm.

#### **2.5 Synthesis and purification of the ibomycin-bodipy conjugate**

The ibomycin-bodipy conjugate was prepared by combining a 5.17 µM solution of ibomycin in DMSO with a slight excess of Bodipy FL-C<sub>5</sub> succinimidyl ester (Life Technologies) and a molar equivalent of triethylamine (Sigma-Aldrich). The reaction was carried out for 12 hours at 4°C. A 25 µL sample of the reaction mixture was subjected to reverse phase HPLC using a C18 semi-preparative column in order to determine if the

reaction was completed. The mobile phases were water (A) and acetonitrile (B), both containing 0.05% formic acid. The method used was as follows 0 to 1 min 54.5% B, a linear gradient from 1 to 11 min up to 71.5% B and from 11 to 12 min up to 100% B, followed by 100% B for 1 min, and then a linear gradient for 1 min down to 54.5% B at a flow rate of 1 ml/min. Absorbance was measured at 220, 266 and 504 nm and a broad peak was observed at approximately 9 minutes. The remainder of reaction mixture was injected onto the column in 25  $\mu$ L injections and the peaks at 9 minutes were collected, pooled, frozen and lyophilized. The dried samples were combined and dissolved in 2 mL of 50% water and acetonitrile before running on HPLC to ensure purity (i.e. a single peak). The pure sample was transferred to a pre-weighed vial and lyophilized once more before being weighed and subsequently dissolved in DMSO generating a 5.12 mg/mL solution.

## 2.6 Fluorescent microscopy

An overnight culture of *S. cerevisiae* BY4741 was diluted to an OD<sub>600</sub> of 0.1 before being further diluted 1:200 into Yeast Nitrogen Base (YNB) medium including appropriate auxotrophic supplements and 2% glucose. The diluted cells were then transferred to a 96-well microtiter plate and incubated at 30°C until they grew to mid-log phase. After addition of the ibomycin-bodipy conjugate at a concentration of 64  $\mu$ g/mL, cells were incubated for 1 hour at 30°C before being harvested, washed and re-suspended in 15  $\mu$ L of ddH<sub>2</sub>O and transferred to a glass slide. Ten microlitres of cooled 1% low-melt agarose was then added to the slide before placing the cover slip and compressing

for 15 minutes. In the case of calcofluor white staining, cells were re-suspended in 0.1 M Tris-HCl buffer (pH 9) before being stained with 2  $\mu$ L of a 3.5 mg/mL solution of Calcofluor white (Sigma-Aldrich) in water. The cells were incubated for 30 minutes with the stain before slide preparation as above. In the case of FM4-64 staining, cells were re-suspended in phosphate buffered saline (PBS) before being stained with 10  $\mu$ L of 0.1 mg/mL FM4-64 (Life Technologies) in water. Cells were then incubated on ice for 3 minutes before slide preparation as above. All slides were visualized using a Leica DMI 6000B widefield microscope at 100X objective under oil immersion and the appropriate filter sets (ibomycin-bodipy: excitation 490 nm, emission 520 nm, calcofluor white: excitation 380 nm, emission 390 nm, FM4-64: excitation 561 nm, emission 600 nm). Images were captured using a Hamamatsu Orca ER-AG camera and Velocity 5.2.0 software. Similar staining protocols were used when visualizing the ibomycin-bodipy conjugate and calcofluor white in *C. neoformans* and *C. albicans*.

## 2.7 Flow cytometry

*C. neoformans* and *C. albicans* cultures were grown in 3 mL of YPD at 30°C overnight before determining cell density using a haemocytometer. Cultures were diluted to a concentration of  $5 \times 10^7$  cells/mL and allowed to grow for 1.5 hours at 30°C before addition of ibomycin-bodipy at a final concentration of 64  $\mu$ g/mL. Cultures were incubated at 30°C for another 45 minutes before being prepared for flow cytometry. Propidium iodide was added at a final concentration of 2  $\mu$ g/mL to appropriate samples which were then incubated on ice for 5 minutes. Cells were pelleted and washed twice

with PBS with 0.1% bovine serum albumin (BSA) before being filtered into cell strainer tubes (BD Falcon, 12x75 mm). All flow cytometry experiments were performed on a BD FACSAria III cell sorter using a 488 nm excitation source and approximately 10,000 events were recorded.

## **2.8 Cell wall damage assay**

Minimal inhibitory concentrations of ibomycin against *S. cerevisiae* (see section 2.2) were determined in the presence and absence of sorbitol. Two-fold dilutions of ibomycin were made in either YPD alone or YPD with 1 M sorbitol before addition of *S. cerevisiae*. Concurrent MICs with caspofungin (positive control) and fluconazole (negative control) were also performed.

## **2.9 Ergosterol feeding experiment**

Ibomycin and ergosterol (dissolved in ethanol) were two-fold serially diluted across the columns and rows of a 96-well microtiter plate (0-128 µg/mL for ibomycin and 0-40 µg/mL for ergosterol) and incubated with *S. cerevisiae* at 30°C for 48 hours. Absorbance was measured at 600 nm and changes in MIC were noted. Amphotericin B (0-128 µg/mL) in combination with ergosterol was used as a positive control.

## **2.10 Chemical genetic screen**

The *Saccharomyces cerevisiae* haploid and heterozygous deletion collections (supplied by the Tyers Lab as two separate pools) were grown in 5 mL of YPD medium

and treated with various concentrations of ibomycin dissolved in DMSO. A 100  $\mu$ L sample from each culture was also transferred to a 96-well microtiter plate to generate growth curves. The 5 mL liquid cultures were incubated at 30°C with shaking for 24 hours. Samples which showed a 10-30% reduction in growth compared to the solvent control (based on the growth curves and optical density of liquid cultures) were selected for genomic DNA (gDNA) extraction. Cells were pelleted and the gDNA was extracted using the Winston-Hoffman glass bead method (75). The purified gDNA was used to amplify the bar-coded tags upstream of the KanMX4 cassette using the various primer combinations (Supplementary table 2). The PCR conditions were as follows: an initial hot start at 98°C for 30 seconds followed by 30 cycles of 98°C for 10 seconds, 54°C for 30 seconds, 72°C for 30 seconds, and a final extension step of 72°C for 10 minutes. The PCR products were then resolved on a 1% agarose gel and the bands at 250 base pairs were excised and purified using a gel extraction kit (Invitrogen). All DNA samples were pooled and sequenced at the Farncombe Metagenomics Facility at McMaster University using the Illumina MiSeq platform and the MiSeq Reagent kit v3 (2 x 75 bp). Counts for each bar-code tag (i.e. strain) were obtained using custom R scripts (by Dr. Michaela Spitzer). Log<sub>2</sub> ratios of counts in ibomycin-treated samples versus control samples were generated for the HIP and HOP assays. The log<sub>2</sub> ratios were normalized by calculating Z-scores. P-values for GO enrichment were calculated based on hypergeometric tests using only genes for which counts were observed in HIP and HOP assays (done by Dr. Michaela Spitzer).

## **Chapter 3: Results**

### **3.1 Ibomycin exhibits fungicidal activity**

An important step in elucidating the mode of action of ibomycin involves determining whether it is a fungistatic or fungicidal agent. To analyze this, a time-kill experiment was performed using *C. neoformans*. Exposure to supra-inhibitory concentrations of ibomycin led to decreased viable cell counts of *C. neoformans* over time. This suggests that ibomycin is acting in a fungicidal manner (Figure 3.1).

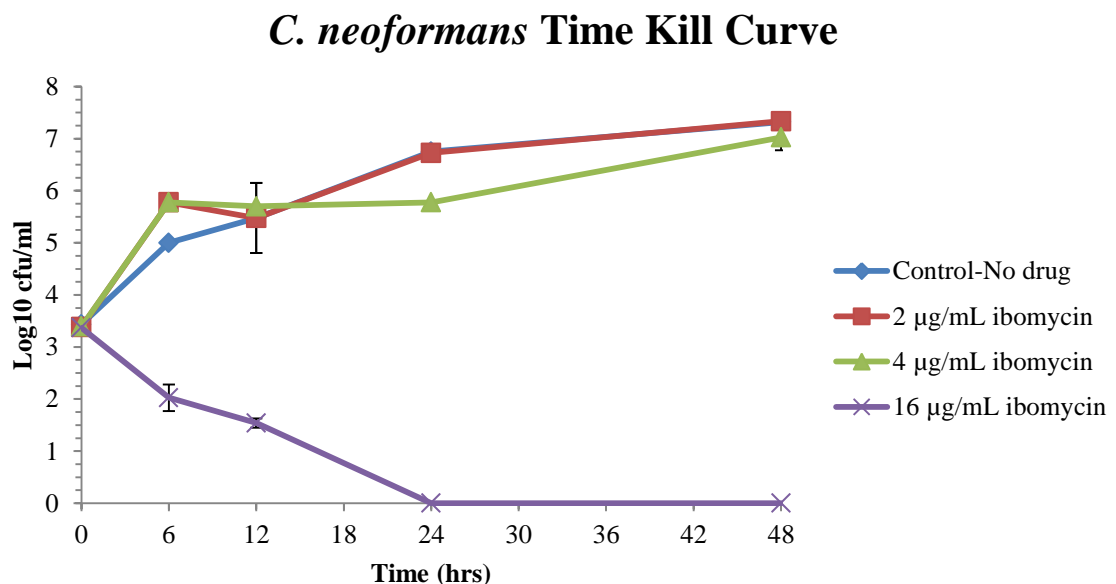


**Figure 3.1: Fungicidal Activity of Ibomycin.** A decrease in CFU/mL over the course of 48 hours suggests that ibomycin is acting in a fungicidal manner. Each experiment was carried out in duplicate.

### **3.2 Ibomycin is hemolytic**

In order to gauge the effectiveness of ibomycin as an antifungal agent in the clinic, its effects on mammalian cells must be tested. A relatively simple means of

identifying cytotoxicity is to determine if ibomycin is hemolytic. Hemolysis occurs as result of compromised membrane structure in erythrocytes. This results in the release of hemoglobin from cells into the supernatant in a sample of blood, which can be measured spectrophotometrically at 541 nm. Ibomycin was hemolytic at all concentrations tested, even as low as 0.25  $\mu\text{g}/\text{mL}$  (Figure 3.2). This was in contrast to amphotericin B, a clinically used polyene known to have toxic effects, which showed considerable hemolytic activity only at concentrations greater than 16  $\mu\text{g}/\text{mL}$ . Devancosamyl ibomycin was 10-fold less toxic to RBCs, causing lysis at concentrations greater than 2  $\mu\text{g}/\text{mL}$ .

### Measure of hemoglobin release in erythrocytes

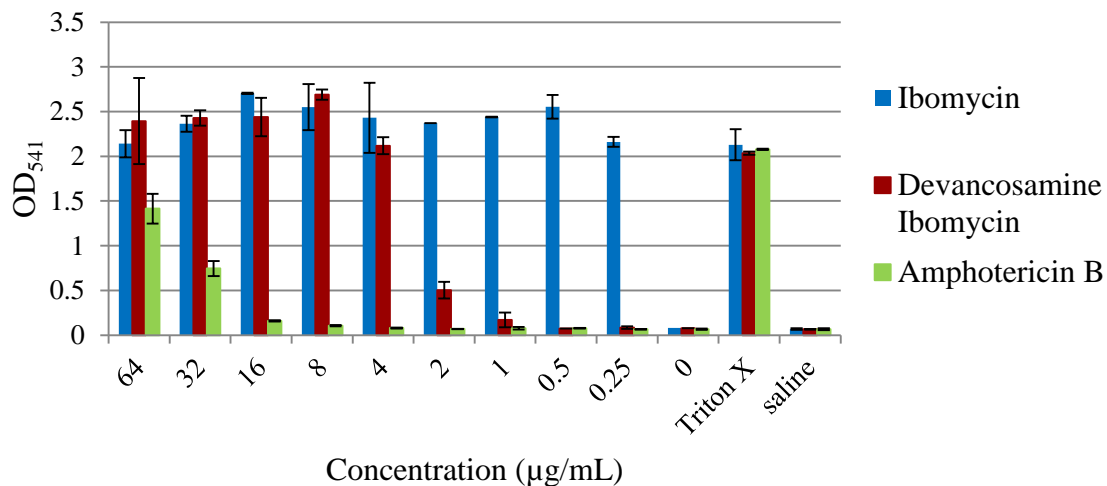


**Figure 3.2: Hemolytic Activity of Ibomycin.** Ibomycin causes RBC lysis at concentrations even as low as 0.25  $\mu\text{g}/\text{mL}$  while devancosamyl ibomycin causes RBC lysis at concentrations greater than 2  $\mu\text{g}/\text{mL}$ . On the X-axis are the concentrations of the compounds tested in  $\mu\text{g}/\text{mL}$  and on the Y-axis are the OD<sub>541</sub> readings of the supernatants. DMSO alone (0  $\mu\text{g}/\text{mL}$  values) was used as a solvent control. Triton X (at 0.1% final concentration) was used as a positive lysis control and saline as a negative control.

### 3.3 Membrane localization of ibomycin-bodipy in *S. cerevisiae*

In order to determine the localization of ibomycin within fungi, a fluorescent analog of ibomycin was synthesized. The succinimidyl ester of bodipy was chemically linked to ibomycin (Figure 3.3) and the conjugate was used to visualize ibomycin localization in *S. cerevisiae* BY4741.

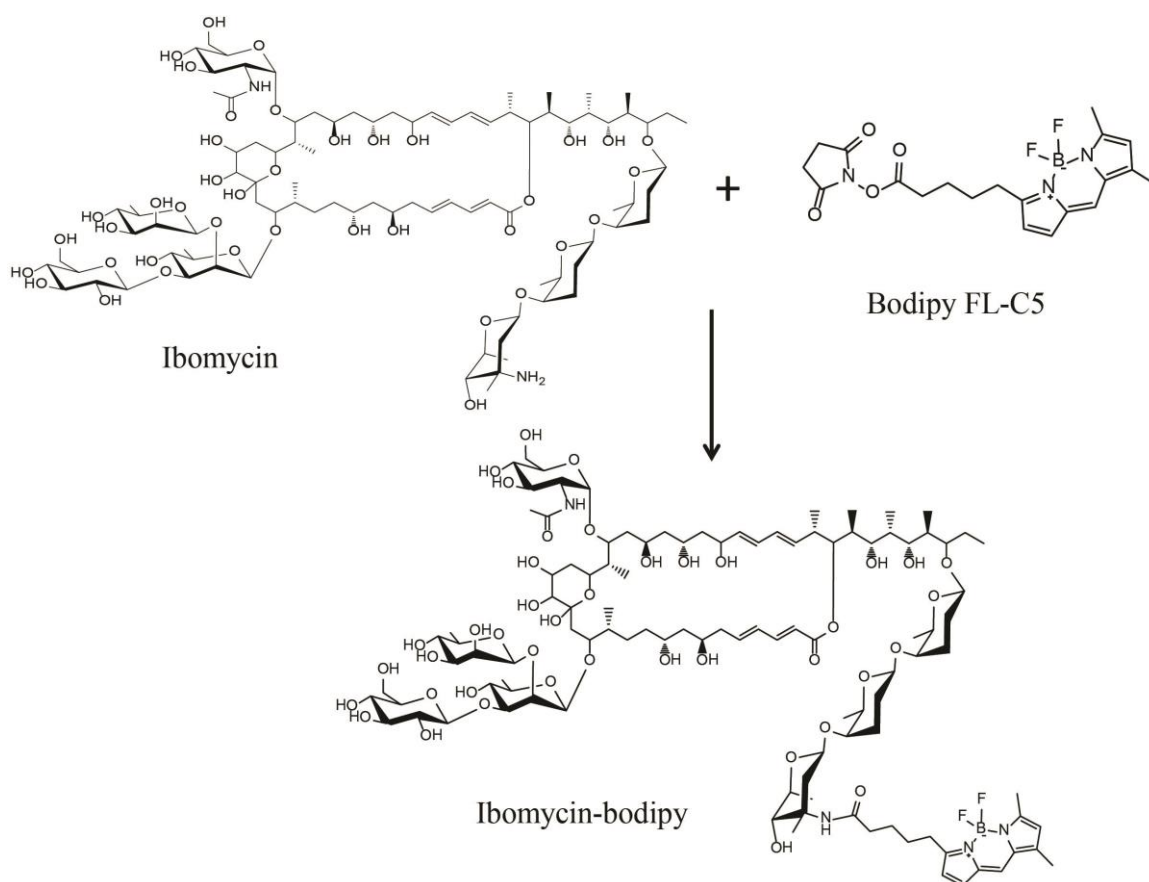


**Figure 3.3: Ibomycin-bodipy synthesis reaction**

Although the ibomycin-bodipy conjugate still retained bioactivity (Table 3.1), its MICs in *S. cerevisiae* BY4741 and *C. neoformans* H99 were higher than ibomycin alone.

**Table 3.1- MICs of ibomycin-bodipy**

	<i>C. neoformans</i> H99	<i>S. cerevisiae</i> BY4741	<i>C. albicans</i> ATCC 92114
Ibomycin	4 µg/mL	8- 16 µg/mL	64 µg/mL
Ibomycin-bodipy	32 µg/mL	32-64 µg/mL	> 128 µg/mL

Treatment of *S. cerevisiae* cells with ibomycin-bodipy resulted in distinct punctate staining patterns that appeared to localize at the periphery of cells (Figure 3.4). This was in contrast to staining with Bodipy-FL C<sub>5</sub> alone which resulted in non-specific staining throughout the cell (Supplementary Figure 5).

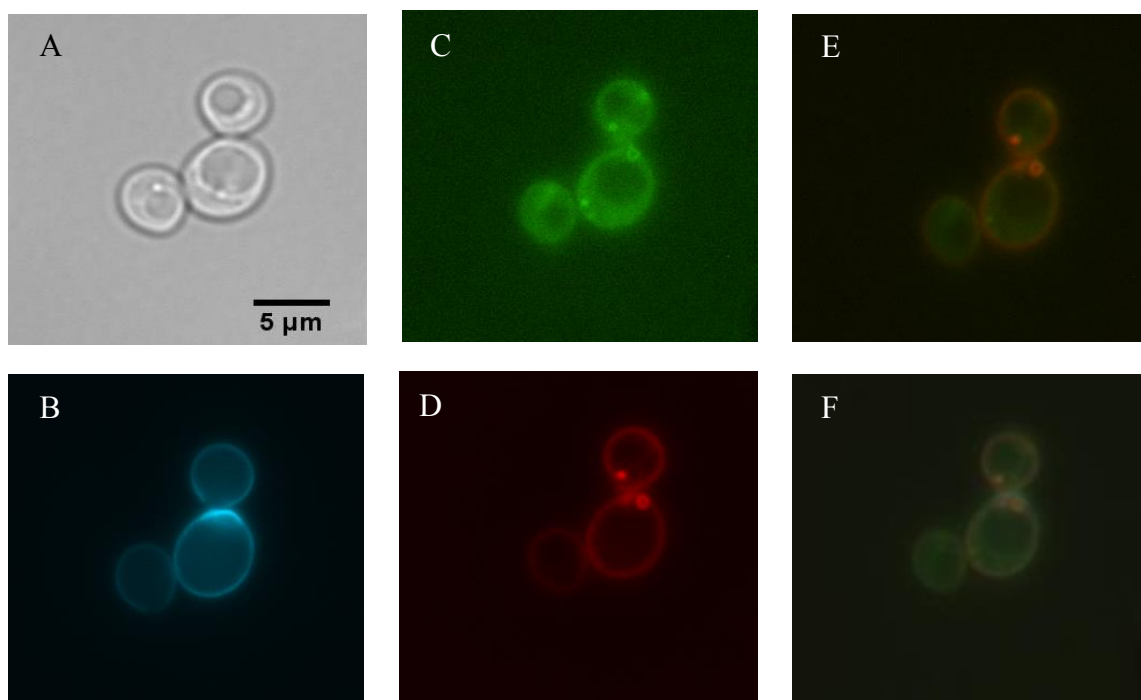


**Figure 3.4: Ibomycin localizes at the cell membrane.** An ibomycin-bodipy conjugate was used to visualize localization of ibomycin in *S. cerevisiae*. Panel (A) is the brightfield image. (B) shows the chitin-rich cell wall of yeast cells stained with calcofluor white. (C) shows cells stained with the ibomycin-bodipy conjugate. (D) shows cells stained with the lipophilic dye FM4-64. (E) shows the overlay image of (C) and (D) while (F) shows the overlay of panels (B), (C) and (D). Concurrent ibomycin-bodipy and FM4-64 staining shows some overlap suggesting that there may be membrane localization of ibomycin. This is also visible in the combined overlay with calcofluor white which can be seen exterior to the stained membrane and ibomycin-bodipy.

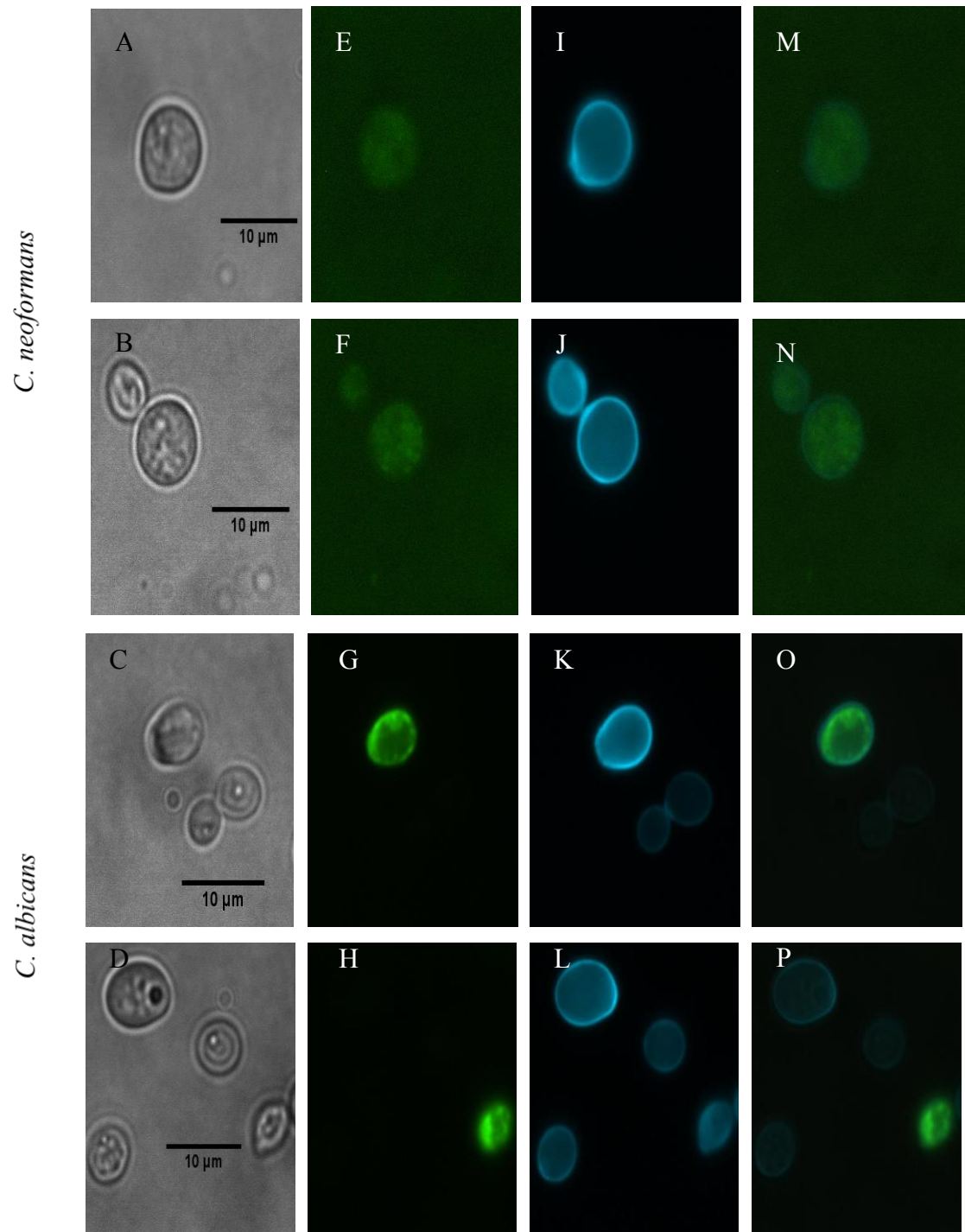
These results suggest that ibomycin exerts its effects at the cell membrane. This result was confirmed upon co-staining *S. cerevisiae* cells with FM4-64, a lipophilic dye used to stain membranes. While FM4-64 alone immediately stained the cell membrane (Figure 3.4, panel D), co-staining revealed that there was some overlap in staining pattern of ibomycin-bodipy and FM4-64 (Figure 3.4, panel E). The cell wall does not seem to be the target as ibomycin-bodipy localization can be seen interior to the calcofluor white stain (Figure 3.4, panel F).

Staining patterns of ibomycin-bodipy in *C. neoformans* and *C. albicans* were not nearly as conclusive. There was variable staining of cells in both organisms with certain cells showcasing membrane localization of the ibomycin-bodipy conjugate while others had little staining or none at all (Figure 3.5).

### 3.4 Flow cytometry

Flow cytometry was used to determine the proportion of *C. neoformans* and *C. albicans* cells stained with ibomycin-bodipy. Cells were also stained with propidium iodide to assess viability and discern whether membrane function was compromised as a result of exposure to ibomycin-bodipy. A comparison with unstained control samples (Supplementary Figure 6) shows that the majority of *C. neoformans* and *C. albicans* cells

**Figure 3.5: Variable ibomycin-bodipy staining patterns in *C. neoformans* and *C. albicans*.** Panels (A) to (D) are brightfield images. Panels (E) to (H) show cells stained with ibomycin-bodipy. Panel (I) to (L) show cells stained with calcofluor white. Panels (M) to (P) show the overlay image of ibomycin-bodipy and calcofluor white. Certain cells show little or no staining with ibomycin-bodipy (F-H). Others display what appears to be either membrane or cell wall staining (M-P), however it is not clear if this is the case.



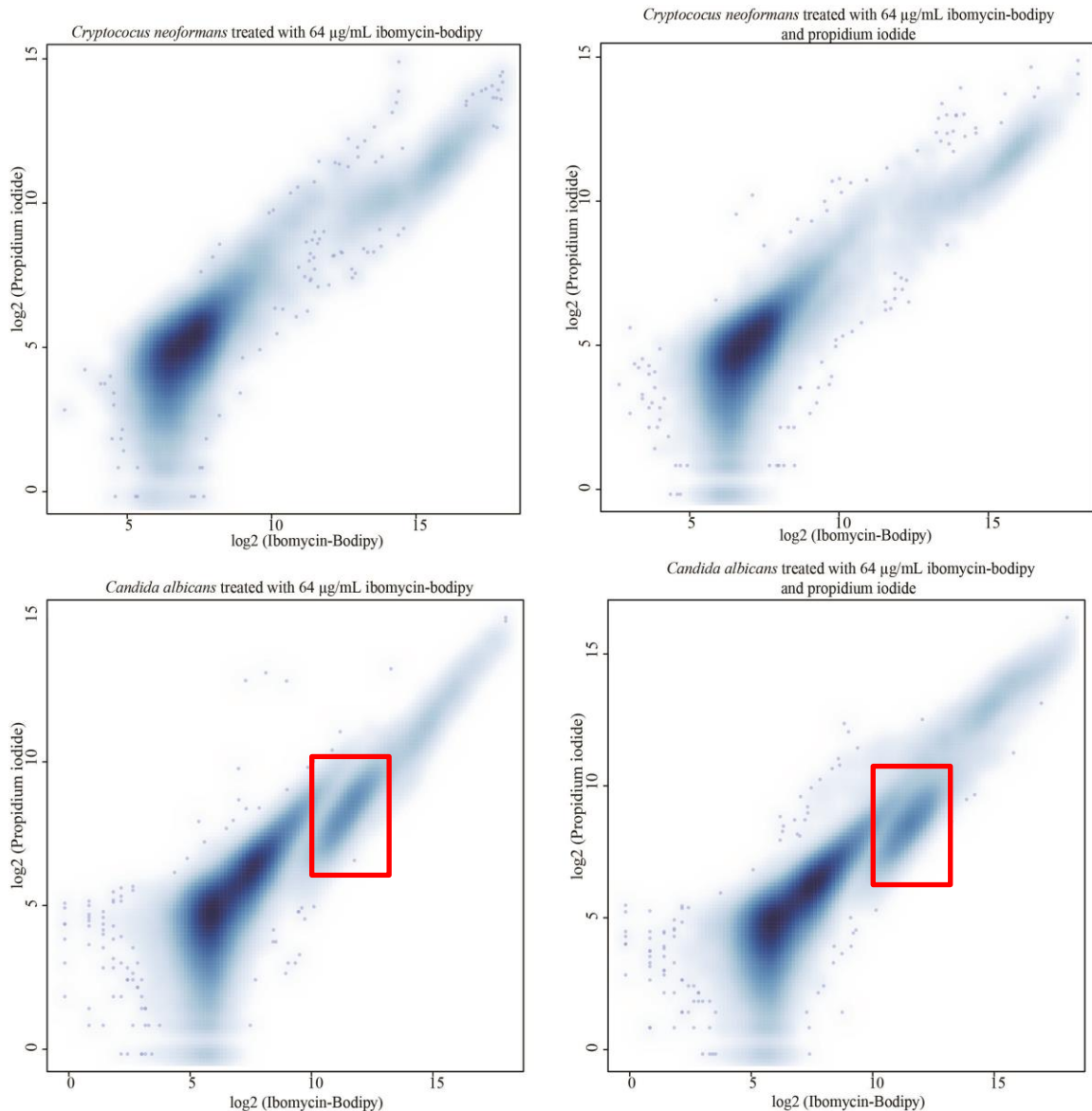


**Figure 3.6: *C. albicans* cells stained with ibomycin-bodipy may not have compromised membranes.** The plots above show the number of cells stained with ibomycin-bodipy and propidium iodide. A majority of cells from both organisms were unstained with either compound. There is a small population of *C. albicans* cells (shown in the red box) that are stained primarily with ibomycin-bodipy but not very much with propidium iodide. No conclusions can be made about ibomycin binding in *C. neoformans*. All axes are set on a logarithmic scale. Areas that are dark blue indicate high density of cells.

treated with ibomycin-bodipy and propidium iodide remained unstained. However, there is a small population of *C. albicans* cells that appear to be stained more with ibomycin-

bodipy but little or no propidium iodide (Figure 3.6). There are no apparent sub-populations in *C. neoformans* cells treated with ibomycin-bodipy and propidium iodide and thus no definite conclusions can be made about ibomycin binding.

### 3.5 Ibomycin does not target the fungal cell wall

In order to confirm that the target of ibomycin was not the fungal cell wall, a sorbitol rescue assay was performed. The cell wall ensures structural integrity of the cell in various environments by regulating osmotic stress. Disruption of the cell wall triggers cell wall stress responses (35) and eventually leads to cell death. However, reports have shown that this phenotype can be reversed in the presence of an osmotic stabilizer such as sorbitol (76). Hence MICs for ibomycin in *S. cerevisiae* were determined with and without sorbitol. Caspofungin, an echinocandin antifungal, had a 4-fold increase in MIC in presence of sorbitol. This was in contrast to ibomycin where the MIC was 16 µg/mL in both conditions (Table 3.2). These results, combined with the microscopy results strongly suggest that the cell wall is not the target of ibomycin.

**Table 3.2-Ibomycin Activity is Undeterred in the presence of Sorbitol**

	MIC (-) Sorbitol	MIC (+) Sorbitol	Fold Increase in MIC
Caspofungin	0.063 µg/mL	0.25 µg/mL	4
Ibomycin	16 µg/mL	16 µg/mL	0

### 3.6 Ibomycin does not have an affinity for sterols

If the cell wall is not the target of ibomycin, then another logical target appears to be the cell membrane based on the results of previous experiments. Fungicidal activity

and hemolysis are signature features of polyene compounds (31) which also have been shown to have a high affinity for sterols as this is fundamental for their mode of action (29, 30). Hence an ergosterol feeding experiment was performed to determine if ibomycin has affinity for sterols (Figure 3.7).

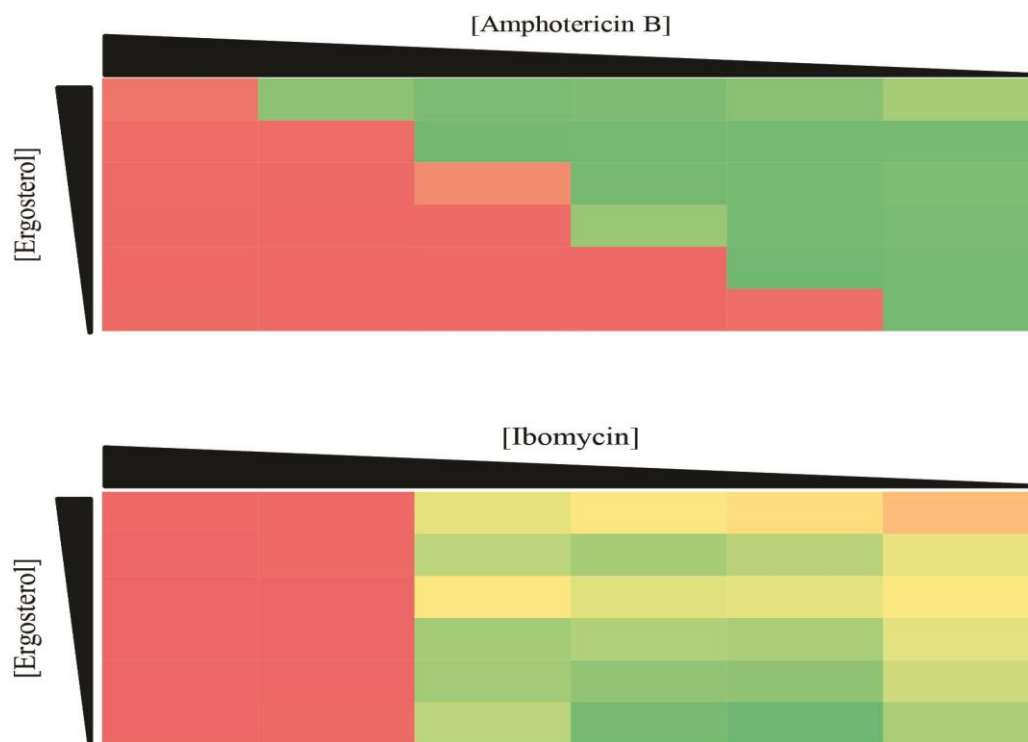


**Figure 3.7: *Ibomycin does not have affinity for sterols.*** The MICs of the polyene amphotericin B and ibomycin were determined in combination with increasing concentrations of ergosterol in *S. cerevisiae*. As the amount of exogenous ergosterol increases, the MIC of amphotericin B also increases. However this is not the case with ibomycin. Concentrations of all compounds are in  $\mu\text{g/mL}$ . Green boxes indicate normal growth while red boxes indicate low growth.

Polyenes such as amphotericin B and nystatin preferentially bind to ergosterol, the fungal equivalent of cholesterol in mammalian membranes. Therefore addition of exogenous ergosterol to cells should result in an increased tolerance to sterol binding compounds (77). In contrast to cells treated with amphotericin B, the MIC of ibomycin

did not change with increasing concentrations of ergosterol. Based on these results, it appears that while ibomycin does appear to be targeting the cell membrane, its mode of action is distinct from that of polyenes.

### **3.7 Yeast Genome Arrays**

The HIP/HOP assay provides a means of determining the target of a compound by revealing deletion strains that are hypersensitive to the compound of interest, in this case, ibomycin. Pools of haploid and heterozygous deletion mutants were grown in YPD medium and treated with various concentrations of ibomycin dissolved in DMSO. Hypersensitive mutants were identified from samples which showed a 10-30% reduction in growth compared to the solvent control after 24 hours (Supplementary Figures 7 and 8). Based on log<sub>2</sub> plots generated for the HIP and HOP assays, there were several mutants from both pools that showed sensitivity to ibomycin. Hits were classified as mutants that had a Z-score less than 2 standard deviations from the mean (i.e. zero). Primary analysis of all candidate genes revealed that they were fairly interrelated in that they were all genes involved in or associated with the secretory pathway. There were a total of 22 hits for the HIP assay with mutants for Sec23, Arp3, Sec14 and TAF proteins being classified as most sensitive (Figure 3.8). Further investigation of enriched genes by gene ontology (GO) processes revealed that they were involved with chromatin modification ( $p = 8.26 \times 10^{-9}$ ), regulation of transcription ( $4.47 \times 10^{-4}$ ) and protein transport ( $2.95 \times 10^{-3}$ ). A full table of p-values can be found in Supplementary Table 3.

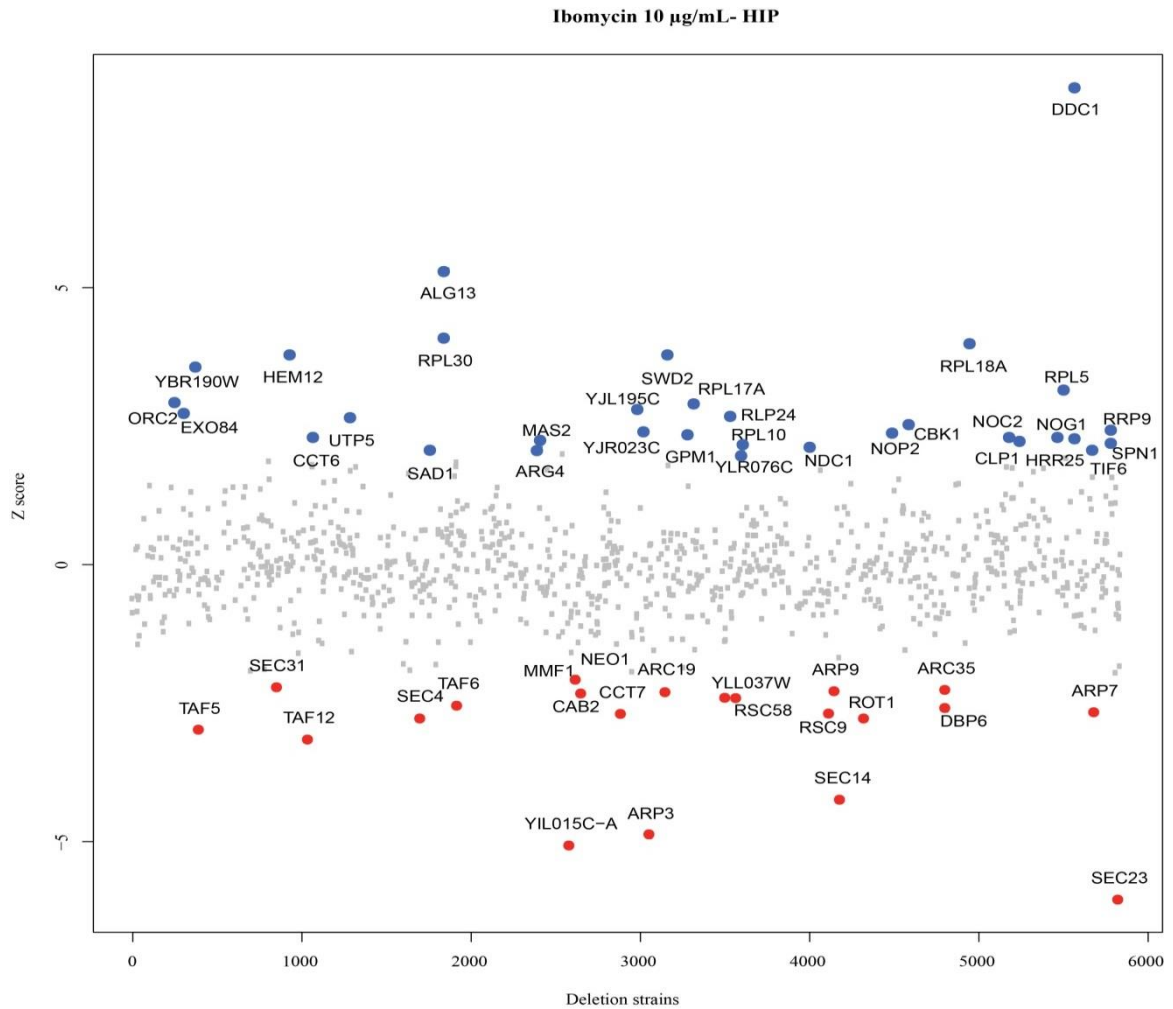


**Figure 3.8:** *Log<sub>2</sub> sensitivity scores of heterozygous deletion mutants to 10  $\mu\text{g}/\text{mL}$  ibomycin.* Log<sub>2</sub> ratios were normalized by calculating Z-scores and outliers were defined as values that were  $\pm 2$  standard deviations from the mean (i.e. zero). Red dots indicate mutants that are sensitive and blue dots indicate mutants that are resistant.

There were 82 hits for the HOP assay, a majority of which were mutants for various components of endosomal sorting complexes required for transport (ESCRT) pathways (Figure 3.9). Common GO processes for the hits included protein transport ( $2.30 \times 10^{-7}$ ), actin cytoskeleton organization ( $5.14 \times 10^{-5}$ ) and lipid transport ( $4.16 \times 10^{-3}$ ) among others (Supplementary Table 4).

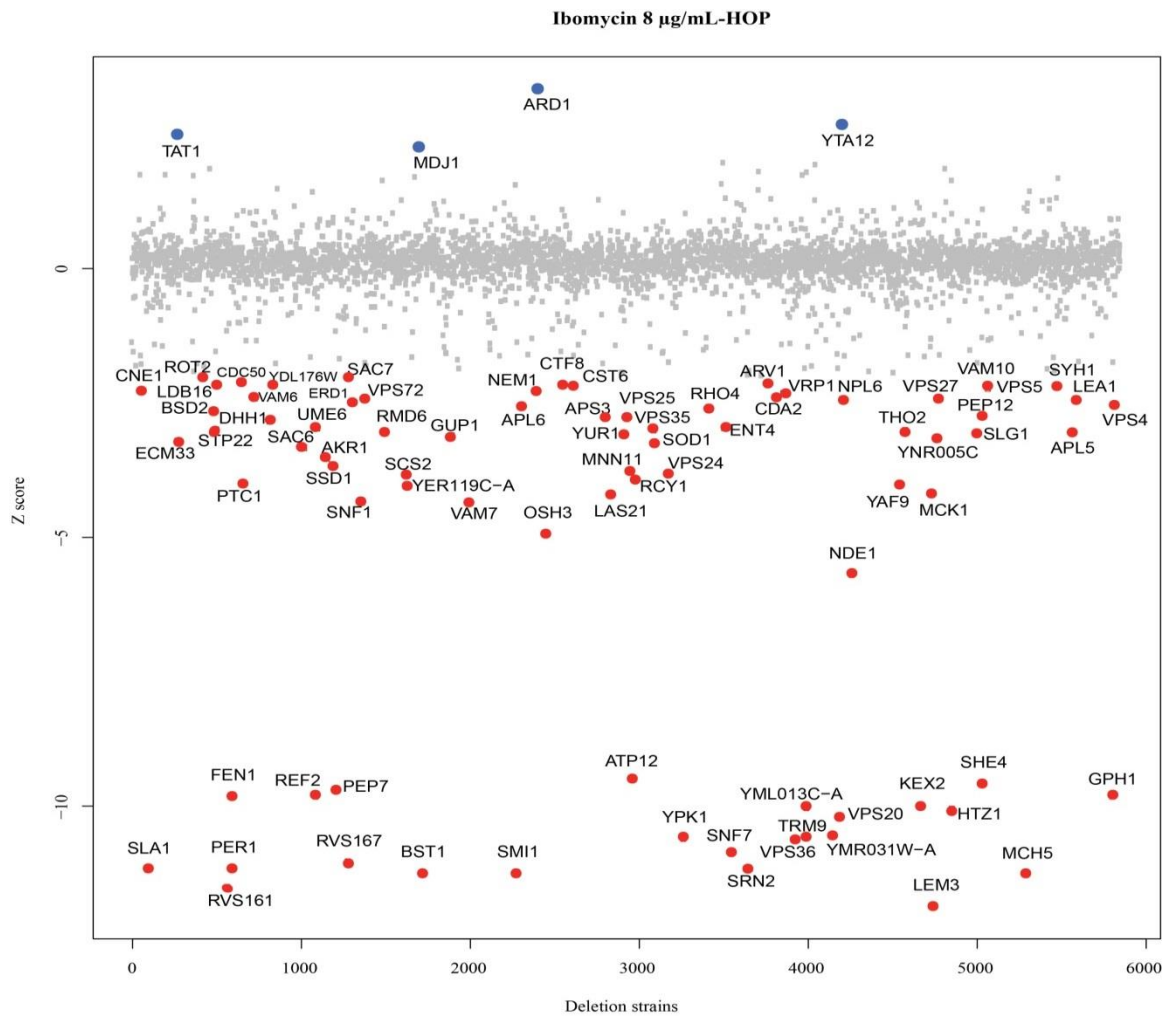


**Figure 3.9: Log<sub>2</sub> sensitivity scores of haploid deletion mutants to 8  $\mu$ g/mL ibomycin.** Log<sub>2</sub> ratios were normalized by calculating Z-scores and outliers were defined as values that were  $\pm 2$  standard deviations from the mean (i.e. zero). Red dots indicate mutants that are sensitive and blue dots indicate mutants that are resistant.

#### **Chapter 4: Discussion**

The data obtained from various mode of action studies suggest that ibomycin impairs cell membrane function in susceptible yeasts. The use of the ibomycin-bodipy conjugate has shown that the compound localizes at the cell membrane and the time kill assay has shown that ibomycin is indeed fungicidal, a property frequently observed for antifungals which target the cell membrane, especially polyenes. The compound is also a very potent cytotoxic agent, demonstrated through hemolysis experiments. These results strongly advocate that ibomycin acts in the same fashion as polyenes. This would not be a complete surprise considering that polyenes have been the prime antifungal compounds isolated from *Streptomyces* species for decades (28). However there are a few facts that don't agree this theory. The first one is apparent by analyzing the structure of ibomycin. To be considered a "polyene", a compound requires a continuous chain of alkene bonds. The feature of the molecule gives it a partially planar structure that is able to interact with the planar ring structures of sterols. The smallest of polyenes, trienenes, have at least three consecutive double bonds (31), whereas ibomycin has two separate sets of conjugated dienes. This leads to the second fact; the structural layout of ibomycin does not permit stable interactions with sterols. This was confirmed with the results of the ergosterol feeding experiment where addition of exogenous ergosterol did not increase tolerance of *S. cerevisiae* to ibomycin. Thus while it appears that ibomycin targets the cell membrane, it seems that it is accomplishing this through a mode of action that is distinct from polyene antifungals.

In order to rule out the cell wall as a possible target, sorbitol rescue assays were performed. Studies have shown that cell wall stress can be reversed in the presence of an osmotic stabilizer such as sorbitol, thereby increasing tolerance to cell wall perturbing agents (78). However, *S. cerevisiae* tolerance to ibomycin did not increase despite addition of 1 M sorbitol, suggesting that ibomycin was not inducing cell wall stress. The absence of ibomycin-bodipy co-localization with the calcofluor stained cell wall also re-affirms this notion. In fact, ibomycin-bodipy staining can be seen interior to and distinctly from the cell wall suggesting that at least in *S. cerevisiae*, ibomycin by-passes the cell wall and targets the cell membrane.

The localization of ibomycin-bodipy could not be determined in either *C. neoformans* or *C. albicans* using fluorescent microscopy due to a lack of consistent staining patterns. Certain cells were totally devoid of staining while others were either stained at the periphery as seen with *S. cerevisiae*. In order to get around this problem, flow cytometry was used to determine if there were significant populations of either organism being stained with ibomycin-bodipy. A sample of cells were also co-stained with propidium iodide to ascertain whether cells were viable and if there was an overlap between cells that were dead and those stained with ibomycin-bodipy. Unfortunately, upon sorting it was found that a majority of the cells were unstained (i.e. the largest population overlapped with the unstained control sample). This is likely due to the fact that ibomycin-bodipy was incubated with the cells for only one hour before sorting. Longer exposure is needed in order to determine whether this observation is an artifact of

the designed protocol. Interestingly, there was a small population amongst the co-stained *C. albicans* cells that appeared to be stained predominantly with ibomycin-bodipy. The fact that they did not take up propidium iodide suggests that membrane function may not be compromised in this population. A plausible theory could be that in *C. albicans*, ibomycin binds to the exterior of the cell but is unable to enter, thereby evading its toxic effects. It would be interesting to see if, after longer incubation with ibomycin-bodipy, there is a shift in population from unstained to stained with only ibomycin-bodipy as this would provide greater evidence for this theory. There were no apparent sub-populations of *C. neoformans* cells and therefore no definite conclusions could be made about the staining patterns in *C. neoformans*. However, a likely prediction is that longer incubation with ibomycin-bodipy will result in the appearance of a population co-stained with ibomycin-bodipy and propidium iodide, if the results in *S. cerevisiae* so far can be recapitulated in *C. neoformans*.

Aside from using conventional target identification methods, the mode of action of ibomycin was also examined using chemical genetics in the form of HIP/HOP. The fact that ibomycin is active against *S. cerevisiae*, allowed for the use of yeast deletion collections for haploinsufficiency and homozygous profiling. The yeast deletion collection is an assortment of deletion strains of all 6000 *S. cerevisiae* genes that have been bar-coded with unique oligonucleotide tags to identify each strain individually (73, 79). Within the collection there are ~1000 heterozygous mutants in which one copy of each of the 1000 essential genes have been replaced with a kanamycin resistance cassette

and unique bar-coded tags. The other 5000 strains are haploid for all other genes and similarly have the functioning copy of the gene replaced with a kanamycin resistance cassette and bar-coded tags. The rationale behind the assay is to examine which heterozygous deletion strains are able to grow in the presence of ibomycin and then amplify and sequence the specific bar-codes to determine which genes are important for fitness in the presence of drug. Genes that buffer the drug target pathway are identified by analyzing hypersensitive haploid deletion mutants. This combined information should provide a better picture of how ibomycin is able to inhibit cell growth.

Of the top 22 hits from the HIP assay, the most sensitive mutants were those that had a single copy of Sec14, Sec 23, Arp3, Taf5 or Taf12. Sec14 is involved in phospholipid transfer (specifically phosphatidylinositol and phosphatidylcholine) between membranes (80). Sec23 is a GTPase-activating protein that acts on Sar1p and is involved in COPII vesicle transfer between the endoplasmic reticulum (ER) and cis-Golgi (81, 82). Arp3 is a component of the Arp2/3 complex, the prime actin nucleation centre in eukaryotic cells (83). Taf5 and Taf12 are components of Transcription Factor II D (TFIID), which associates with RNA polymerase II as a transcription initiation complex (84). Aside from the Taf proteins, the other genes are primarily involved in regulation of membrane structures associated with the secretory pathway. This was also a common feature of a majority the 82 hits from the HOP assay which were involved in vesicle formation and transport from the ER to the membrane and extracellular space. The results of the HIP/HOP assay indirectly suggest membrane disruption as a result of exposure to

ibomycin. Protein transport and vesicular trafficking to the cell membrane are important cellular processes and thus membrane disruption would undoubtedly have detrimental effects on these processes. These results also reveal that there is no single protein/enzyme target of ibomycin.

### **Future Directions**

While there is evidence that ibomycin is amongst a class of antifungals that are membrane disruptors (but not polyenes), there is still uncertainty with respect to the downstream effects of membrane perturbation by ibomycin (i.e. if specific ions or metabolites are released). It is unknown if ibomycin causes  $K^+$  leakage in fungi. An attempt to measure potassium ion release from ibomycin-treated yeast cells was made using PBFI, a fluorescent dye that binds potassium ions (85), however significant changes could not be detected. There are other dyes for assaying leakage of other ions from cells such as CoroNa green for  $Na^+$  or lucigenin for  $Cl^-$  (86, 87). Alternatively, the measure of release of UV-absorbing materials such as nucleotides could be used to verify membrane damage.

Another avenue to explore is determining which structural moieties of ibomycin are required for its bioactivity. The multitude of sugars on the ibomycin aglycone make it one of the largest molecules to come out the WAC collection, however the purpose of so many tailoring events is not well understood. The discovery of an active analog lacking the vancosamine sugar has already been found and shown to be less toxic to mammalian cells than ibomycin. It would be interesting to see if removal of more sugars allows

ibomycin to retain its selective bioactivity or even broadens it to include *C. albicans*. It may be possible that *C. albicans* is unable to recognize a naked ibomycin analog and thus cannot prevent absorption of the molecule by its cell membrane. *C. albicans* is known to have extracellular lectins that recognize sugars such as N-acetyl glucosamine (88). However the challenging aspect of this investigation remains obtaining or purifying these sugarless analogs. Chemical cleavage of sugars using acid hydrolysis risks opening the lactone ring that holds the backbone together. On the other hand, genetic manipulation of WAC 2288 to knock out the glycosyltransferases in the ibomycin cluster has proven to be a difficult task. While WAC 2288 is willing to accept foreign vectors via conjugation, it seems that it has poor homologous recombination machinery, evident from the extremely low number of exconjugants obtained. A possible solution would be to generate miniature cosmids with long arms of homology in order to promote recombination.

## **Conclusion**

This work has attempted to identify the mode of action of ibomycin through traditional and genetic approaches. Based on the available data, the following conclusions can be made about the mode of action of ibomycin. There is strong evidence to suggest that it is not associated with cell wall biosynthesis based on localization and absence of viability rescue in presence of sorbitol. Despite having characteristics associated with membrane perturbing agents (cidality, hemolysis and even membrane localization), it does not seem that ibomycin is exerting its effects in the same manner as polyenes which

typically show strong affinity for sterols. The results of the HIP/HOP assays suggest that is no single protein target for ibomycin, but rather that ibomycin's actions have downstream effects that impair vesicular trafficking and protein transport. Finally, it is predicted that *C. albicans* is able to evade the toxic effects of ibomycin as a result of simply preventing access to its cell membrane. The significance of this work lies in the discovery of a potentially unique means of targeting a crucial feature of fungal biology. Ibomycin now has a face to its name, figuratively speaking, in that we now have a better understanding of the selective bioactivity of this novel antifungal compound.

**References:**

1. Brown, G. D., et al. (2012). Hidden killers: human fungal infections. *Sci Transl Med* **4**(165):165rv13.
2. Tlamcani, Z., and Er-rami, M. (2013). Fungal opportunist infection: Common and emerging fungi in immunocompromised patients. *J Immun Tech Infect Dis* **2**:1-5.
3. Knoke, M., and Schwesinger, G. (1994). One hundred years ago: the history of cryptococcosis in Greifswald. *Medical mycology in the nineteenth century. Mycoses* **37**(7-8):229-33.
4. Sanfelice, F. (1895). Sull'azione patogena dei bastomiceti. *Ann Inst Igien Univ Roma* **5**:239-262.
5. Lupi, O., Tying, S. K., and McGinnis, M. R. (2005). Tropical dermatology: fungal tropical diseases. *J Am Acad Dermatol* **53**(6):931-51, quiz 952-4.
6. Park, B. J., et al. (2009). Estimation of the current global burden of cryptococcal meningitis among persons living with HIV/AIDS. *AIDS* **23**(4):525-30.
7. Chowdhary, A., Rhandhawa, H. S., Prakash, A., and Meis, J. F. (2012). Environmental prevalence of *Cryptococcus neoformans* and *Cryptococcus gattii* in India: an update. *Crit Rev Microbiol* **38**(1):1-16.
8. Liu, T. B., Perlin, D. S., and Xue, C. (2012). Molecular mechanisms of cryptococcal meningitis. *Virulence* **3**(2):173-81.
9. Kechichian, T. B., Shea, J., and Del Poeta, M. (2007). Depletion of alveolar macrophages decreases the dissemination of a glucosylceramide-deficient mutant of *Cryptococcus neoformans* in immunodeficient mice. *Infect Immun* **75**(10):4792-8.
10. Doering, T. L. (2009). How sweet it is! Cell wall biogenesis and polysaccharide capsule formation in *Cryptococcus neoformans*. *Annu Rev Microbiol* **63**:223-47.
11. Vecchiarelli, A., and Monari, C. (2012). Capsular Material of *Cryptococcus neoformans*: Virulence and Much More. *Mycopathologia*.
12. Nosanchuk, J. D., and Casadevall, A. (2006). Impact of melanin on microbial virulence and clinical resistance to antimicrobial compounds. *Antimicrob Agents Chemother* **50**(11):3519-28.
13. Hippocrates. Of the Epidemics Book II. Translated by: F. Adams. The Internet Classics Archive. Curated by: D. C. Stevenson. [Online.]
14. Barnett, J. A. (2008). A history of research on yeasts 12: medical yeasts part 1, *Candida albicans*. *Yeast* **25**(6):385-417.
15. Zhu, W., and Filler, S. G. (2010). Interactions of *Candida albicans* with epithelial cells. *Cell Microbiol* **12**(3):273-82.
16. Staab, J. F., Bradway, S. D., Fidel, P. L., and Sundstrom, P. (1999). Adhesive and mammalian transglutaminase substrate properties of *Candida albicans* Hwp1. *Science* **283**(5407):1535-8.
17. Enoch, D. A., Ludlam, H. A., and Brown, N. M. (2006). Invasive fungal infections: a review of epidemiology and management options. *J Med Microbiol* **55**(Pt 7):809-18.

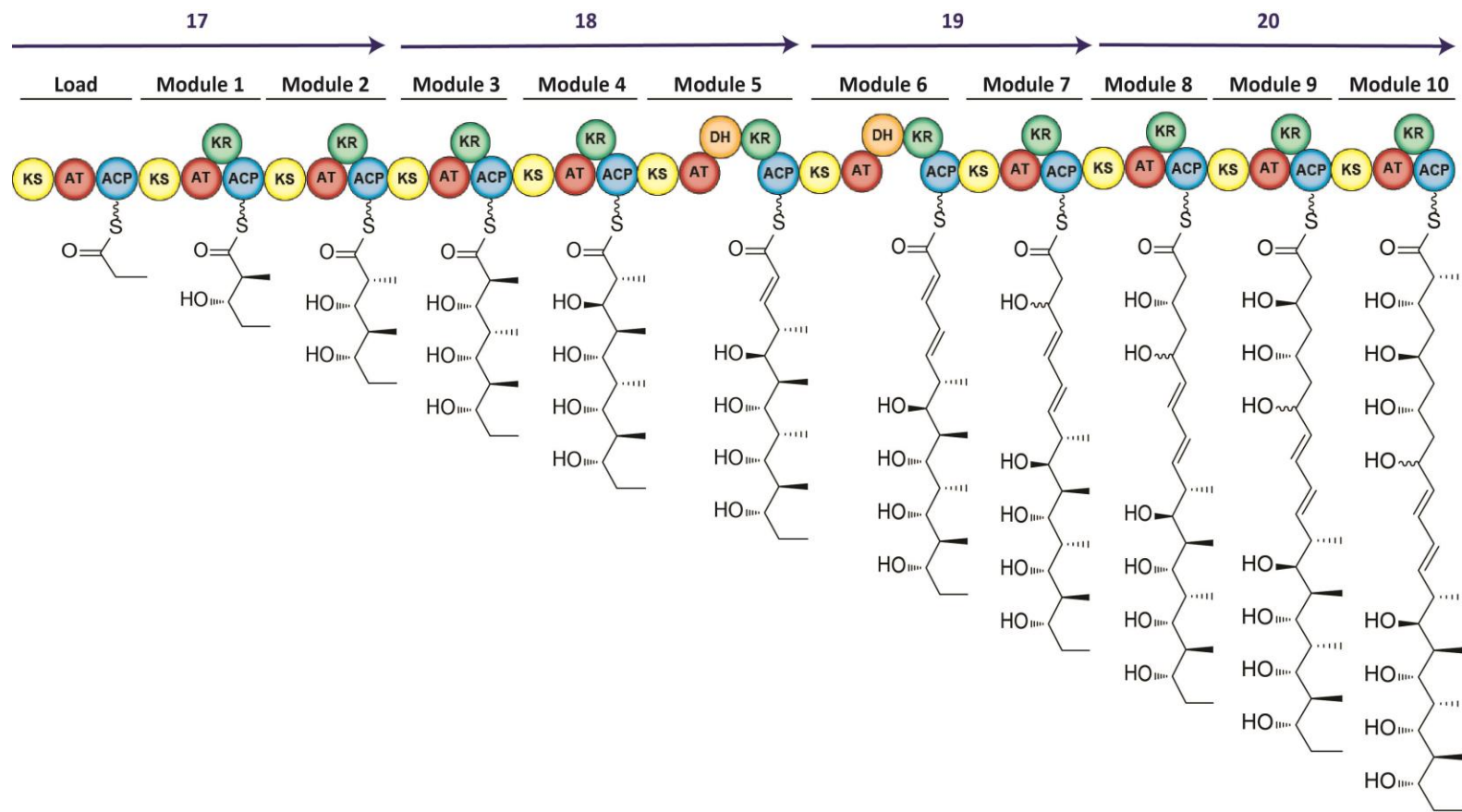
18. Sudbery, P. E. (2011). Growth of *Candida albicans* hyphae. *Nat Rev Microbiol* **9**(10):737-48.
19. Andriole, V. T. (1999). The 1998 Garrod lecture. Current and future antifungal therapy: new targets for antifungal agents. *J Antimicrob Chemother* **44**(2):151-62.
20. Sheehan, D. J., Hitchcock, C. A., and Sibley, C. M. (1999). Current and emerging azole antifungal agents. *Clin Microbiol Rev* **12**(1):40-79.
21. Lupetti, A., et al. (2002). Molecular basis of resistance to azole antifungals. *Trends Mol Med* **8**(2):76-81.
22. Posteraro, B., et al. (2003). Identification and characterization of a *Cryptococcus neoformans* ATP binding cassette (ABC) transporter-encoding gene, CnAFR1, involved in the resistance to fluconazole. *Mol Microbiol* **47**(2):357-71.
23. Coste, A. T., et al. (2004). TAC1, transcriptional activator of CDR genes, is a new transcription factor involved in the regulation of *Candida albicans* ABC transporters CDR1 and CDR2. *Eukaryot Cell* **3**(6):1639-52.
24. Schubert, S., Popp, C., Rogers, P. D., and Morschhauser, J. (2011). Functional dissection of a *Candida albicans* zinc cluster transcription factor, the multidrug resistance regulator Mrr1. *Eukaryot Cell* **10**(8):1110-21.
25. Wang, H., et al. (2009). Rapid detection of ERG11 gene mutations in clinical *Candida albicans* isolates with reduced susceptibility to fluconazole by rolling circle amplification and DNA sequencing. *BMC Microbiol* **9**:167.
26. Favre, B., Didmon, M., and Ryder, N. S. (1999). Multiple amino acid substitutions in lanosterol 14 $\alpha$ -demethylase contribute to azole resistance in *Candida albicans*. *Microbiology* **145**(10):2715-25.
27. Xu, Y., Chen, L., and Li, C. (2008). Susceptibility of clinical isolates of *Candida* species to fluconazole and detection of *Candida albicans* ERG11 mutations. *J Antimicrob Chemother* **61**(4):798-804.
28. Oroshnik, W., and Mebane, A. (1963). The polyene antifungal antibiotics, p. 17-79, Progress in the Chemistry of Organic Natural Products/Progrès Dans La Chimie Des Substances Organiques Naturelles. Springer.
29. Neumann, A., Baginski, M., and Czub, J. (2010). How do sterols determine the antifungal activity of amphotericin B? Free energy of binding between the drug and its membrane targets. *J Am Chem Soc* **132**(51):18266-72.
30. Gray, K. C., et al. (2012). Amphotericin primarily kills yeast by simply binding ergosterol. *Proc Natl Acad Sci U S A* **109**(7):2234-9.
31. Kotler-Brajtburg, J., et al. (1979). Classification of polyene antibiotics according to chemical structure and biological effects. *Antimicrob Agents Chemother* **15**(5):716-22.
32. Sheikh, S., et al. (2010). Nanosomal Amphotericin B is an efficacious alternative to Ambisome for fungal therapy. *Int J Pharm* **397**(1-2):103-8.
33. Free, S. J. (2013). Fungal cell wall organization and biosynthesis. *Adv Genet* **81**:33-82.

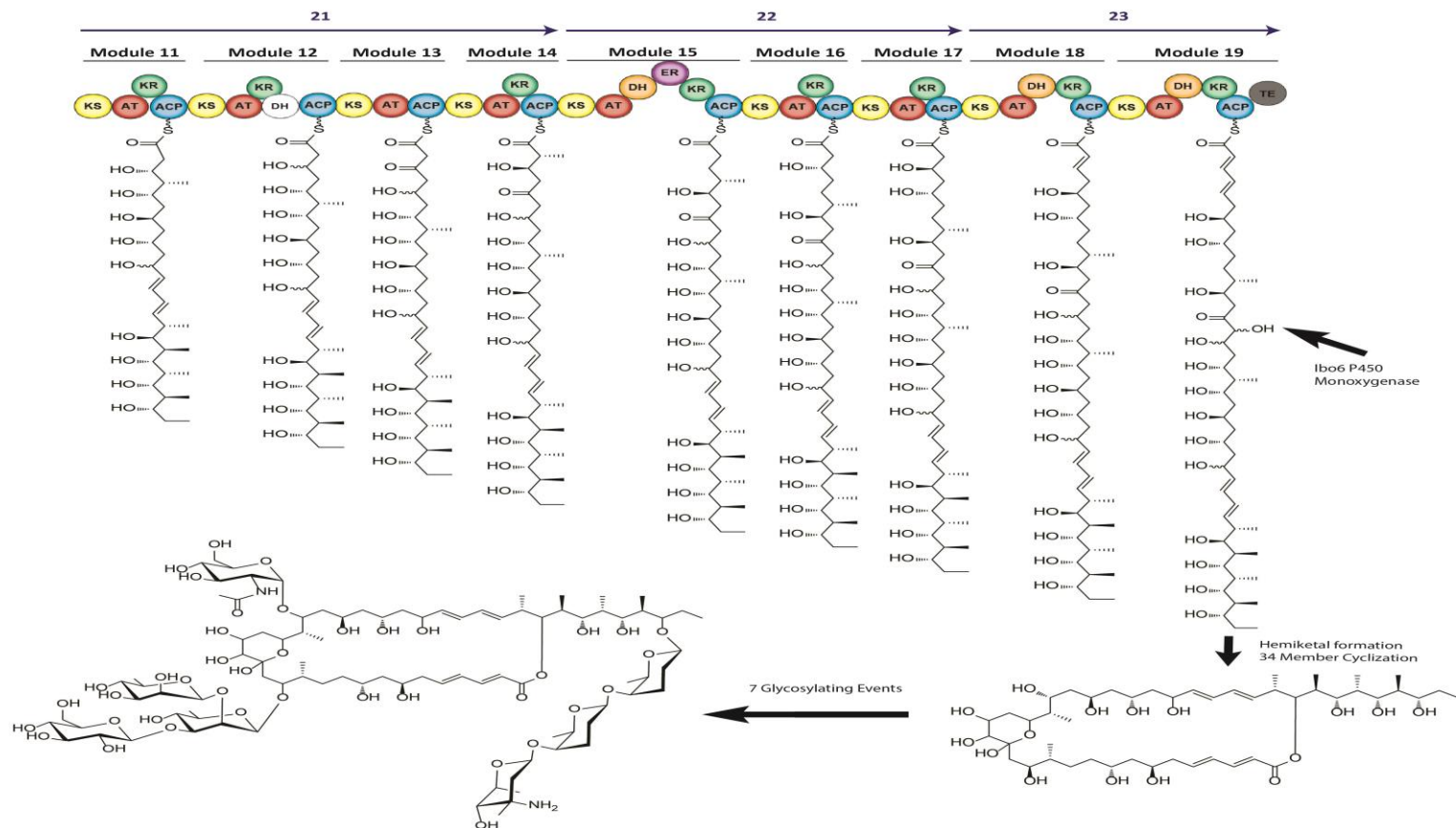
34. Balkovec, J. M., et al. (2014). Discovery and development of first in class antifungal caspofungin (CANCIDAS(R))--a case study. *Nat Prod Rep* **31**(1):15-34.
35. Shapiro, R. S., Robbins, N., and Cowen, L. E. (2011). Regulatory circuitry governing fungal development, drug resistance, and disease. *Microbiol Mol Biol Rev* **75**(2):213-67.
36. Maligie, M. A., and Selitrennikoff, C. P. (2005). Cryptococcus neoformans resistance to echinocandins: (1,3)beta-glucan synthase activity is sensitive to echinocandins. *Antimicrob Agents Chemother* **49**(7):2851-6.
37. Perlin, D. S. (2007). Resistance to echinocandin-class antifungal drugs. *Drug Resist Updat* **10**(3):121-30.
38. Perea, S., and Patterson, T. F. (2002). Antifungal resistance in pathogenic fungi. *Clin Infect Dis* **35**(9):1073-80.
39. Ghannoum, M. A., and Rice, L. B. (1999). Antifungal agents: mode of action, mechanisms of resistance, and correlation of these mechanisms with bacterial resistance. *Clin Microbiol Rev* **12**(4):501-17.
40. Hopwood, D. A. (2007). *Streptomyces in Nature and Medicine: The Antibiotic Makers*. Oxford University Press, New York.
41. Fenical, W., and Jensen, P. R. (2006). Developing a new resource for drug discovery: marine actinomycete bacteria. *Nat Chem Biol* **2**(12):666-73.
42. Garrity, G. M., Heimbuch, B. K., and Gagliardi, M. (1996). Isolation of zoosporogenous actinomycetes from desert soils. *J Industrial Microbiology* **17**:260-267.
43. Mevs, U., et al. (2000). *Modestobacter multiseptatus* gen. nov., sp. nov., a budding actinomycete from soils of the Asgard Range (Transantarctic Mountains). *Int J Syst Evol Microbiol* **50**(1):337-46.
44. Paramageetham, C., Reddy, A., and Babu, G. P. (2013). Biocatalytic potentials of actinomycetes dwelling in hypersaline environments. *Asian J Exp Biol Sci* **4**(1):152-154.
45. Allen, H. K., et al. (2010). Call of the wild: antibiotic resistance genes in natural environments. *Nat Rev Microbiol* **8**(4):251-9.
46. Payne, D. J., Gwynn, M. N., Holmes, D. J., and Pompliano, D. L. (2007). Drugs for bad bugs: confronting the challenges of antibacterial discovery. *Nat Rev Drug Discov* **6**(1):29-40.
47. Wright, G. D. (2012). Antibiotics: a new hope. *Chem Biol* **19**(1):3-10.
48. Challis, G. L. (2008). Mining microbial genomes for new natural products and biosynthetic pathways. *Microbiology* **154**(Pt 6):1555-69.
49. Craney, A., Ahmed, S., and Nodwell, J. (2013). Towards a new science of secondary metabolism. *J Antibiot (Tokyo)* **66**(7):387-400.
50. Yu, H., et al. (2010). Recent developments and future prospects of antimicrobial metabolites produced by endophytes. *Microbiol Res* **165**(6):437-49.
51. Bacon, C. W., and White, J. (2000). *Microbial Endophytes*. Taylor & Francis.

52. Strobel, G., and Daisy, B. (2003). Bioprospecting for microbial endophytes and their natural products. *Microbiol Mol Biol Rev* **67**(4):491-502.
53. Marmann, A., et al. (2014). Co-cultivation--a powerful emerging tool for enhancing the chemical diversity of microorganisms. *Mar Drugs* **12**(2):1043-65.
54. Rateb, M. E., et al. (2013). Induction of diverse secondary metabolites in *Aspergillus fumigatus* by microbial co-culture. *RSC Advances* **3**(34):14444-14450.
55. Schroeckh, V., et al. (2009). Intimate bacterial-fungal interaction triggers biosynthesis of archetypal polyketides in *Aspergillus nidulans*. *Proc Natl Acad Sci U S A* **106**(34):14558-63.
56. O'Brien, J. S. (2012). Discovery and Characterization of ibomycin: an anticryptococcal metabolite produced by WAC 2288. Open Dissertations and Theses. McMaster University, Hamilton.
57. Medema, M. H., et al. (2011). antiSMASH: rapid identification, annotation and analysis of secondary metabolite biosynthesis gene clusters in bacterial and fungal genome sequences. *Nucleic Acids Res* **39**(Web Server issue):W339-46.
58. Staunton, J., and Weissman, K. J. (2001). Polyketide biosynthesis: a millennium review. *Nat Prod Rep* **18**(4):380-416.
59. Yadav, G., Gokhale, R. S., and Mohanty, D. (2003). Computational approach for prediction of domain organization and substrate specificity of modular polyketide synthases. *J Mol Biol* **328**(2):335-63.
60. Weissman, K. J. (2009). Introduction to polyketide biosynthesis. *Methods Enzymol* **459**:3-16.
61. Keatinge-Clay, A. T. (2007). A tylosin ketoreductase reveals how chirality is determined in polyketides. *Chem Biol* **14**(8):898-908.
62. Tang, L., Yoon, Y. J., Choi, C. Y., and Hutchinson, C. R. (1998). Characterization of the enzymatic domains in the modular polyketide synthase involved in rifamycin B biosynthesis by *Amycolatopsis mediterranei*. *Gene* **216**(2):255-65.
63. Anand, S., et al. (2010). SBSPKS: structure based sequence analysis of polyketide synthases. *Nucleic Acids Res* **38**(Web Server issue):W487-96.
64. Chen, Y. L., et al. (2012). Identification of phoslactomycin biosynthetic gene clusters from *Streptomyces platensis* SAM-0654 and characterization of PnR1 and PnR2 as positive transcriptional regulators. *Gene* **509**(2):195-200.
65. Takaishi, M., Kudo, F., and Eguchi, T. (2013). Identification of the incednine biosynthetic gene cluster: characterization of novel beta-glutamate-beta-decarboxylase IdnL3. *J Antibiot (Tokyo)* **66**(12):691-9.
66. Hoffmeister, D., et al. (2000). The NDP-sugar co-substrate concentration and the enzyme expression level influence the substrate specificity of glycosyltransferases: cloning and characterization of deoxysugar biosynthetic genes of the urdamycin biosynthetic gene cluster. *Chem Biol* **7**(11):821-31.
67. Ichinose, K., et al. (1998). The granaticin biosynthetic gene cluster of *Streptomyces violaceoruber* Tu22: sequence analysis and expression in a heterologous host. *Chem Biol* **5**(11):647-59.

68. Zhang, X., et al. (2008). Biosynthetic investigations of lactonamycin and lactonamycin z: cloning of the biosynthetic gene clusters and discovery of an unusual starter unit. *Antimicrob Agents Chemother* **52**(2):574-85.
69. Chen, H., et al. (2000). Deoxysugars in glycopeptide antibiotics: enzymatic synthesis of TDP-L-epivancosamine in chloroeremomycin biosynthesis. *Proc Natl Acad Sci U S A* **97**(22):11942-7.
70. Madduri, K., Waldron, C., and Merlo, D. J. (2001). Rhamnose biosynthesis pathway supplies precursors for primary and secondary metabolism in *Saccharopolyspora spinosa*. *J Bacteriol* **183**(19):5632-8.
71. Donadio, S., et al. (2005). Comparative analysis and insights into the evolution of gene clusters for glycopeptide antibiotic biosynthesis. *Mol Genet Genomics* **274**(1):40-50.
72. Cong, F., Cheung, A. K., and Huang, S. M. (2012). Chemical genetics-based target identification in drug discovery. *Annu Rev Pharmacol Toxicol* **52**:57-78.
73. Giaever, G., et al. (2002). Functional profiling of the *Saccharomyces cerevisiae* genome. *Nature* **418**(6896):387-91.
74. NCCLS. (2008). Reference method for broth dilution antifungal susceptibility testing of yeasts. Approved standard M27-A3, Wayne, Pennsylvania.
75. Hoffman, C. S., and Winston, F. (1987). A ten-minute DNA preparation from yeast efficiently releases autonomous plasmids for transformation of *Escherichia coli*. *Gene* **57**(2-3):267-72.
76. Onishi, J., et al. (2000). Discovery of novel antifungal (1,3)-beta-D-glucan synthase inhibitors. *Antimicrob Agents Chemother* **44**(2):368-77.
77. Carrasco, H., et al. (2012). Antifungal activity of eugenol analogues. Influence of different substituents and studies on mechanism of action. *Molecules* **17**(1):1002-24.
78. Cassone, A., Mason, R. E., and Kerridge, D. (1981). Lysis of growing yeast-form cells of *Candida albicans* by echinocandin: a cytological study. *Sabouraudia* **19**(2):97-110.
79. Giaever, G., et al. (1999). Genomic profiling of drug sensitivities via induced haploinsufficiency. *Nat Genet* **21**(3):278-83.
80. Bankaitis, V. A., Malehorn, D. E., Emr, S. D., and Greene, R. (1989). The *Saccharomyces cerevisiae* SEC14 gene encodes a cytosolic factor that is required for transport of secretory proteins from the yeast Golgi complex. *J Cell Biol* **108**(4):1271-81.
81. Barlowe, C., et al. (1994). COPII: a membrane coat formed by Sec proteins that drive vesicle budding from the endoplasmic reticulum. *Cell* **77**(6):895-907.
82. Yoshihisa, T., Barlowe, C., and Schekman, R. (1993). Requirement for a GTPase-activating protein in vesicle budding from the endoplasmic reticulum. *Science* **259**(5100):1466-8.
83. Machesky, L. M., and Gould, K. L. (1999). The Arp2/3 complex: a multifunctional actin organizer. *Curr Opin Cell Biol* **11**(1):117-21.

84. Green, M. R. (2000). TBP-associated factors (TAFII)s: multiple, selective transcriptional mediators in common complexes. *Trends Biochem Sci* **25**(2):59-63.
85. Negulescu, P. A., and Machen, T. E. (1990). Intracellular ion activities and membrane transport in parietal cells measured with fluorescent dyes. *Methods Enzymol* **192**:38-81.
86. Geddes, C. D., Apperson, K., Karolin, J., and Birch, D. J. (2001). Chloride-sensitive fluorescent indicators. *Anal Biochem* **293**(1):60-6.
87. Meier, S. D., Kovalchuk, Y., and Rose, C. R. (2006). Properties of the new fluorescent Na<sup>+</sup> indicator CoroNa Green: comparison with SBFI and confocal Na<sup>+</sup> imaging. *J Neurosci Methods* **155**(2):251-9.
88. Alonso, R., et al. (2001). Different adhesins for type IV collagen on *Candida albicans*: identification of a lectin-like adhesin recognizing the 7S(IV) domain. *Microbiology* **147**(Pt 7):1971-81.

**Appendix**



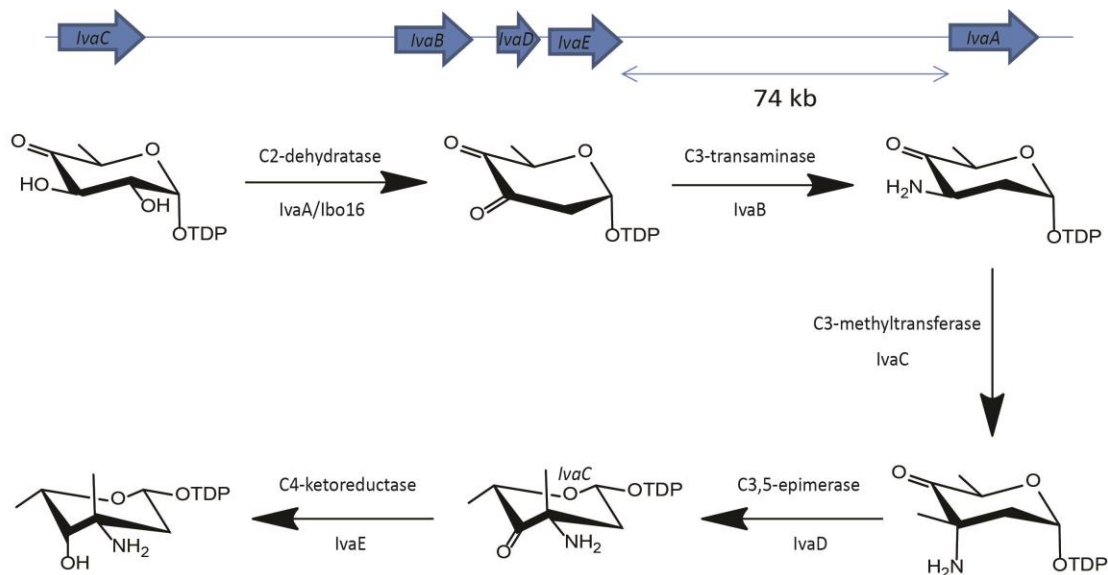
**Supplementary Figure 1: Model for Ibomycin Biosynthesis.** Modular biosynthesis of ibomycin according to the catalytic domains encoded by the PKS genes. Annotated *ibo* genes are displayed above blue arrows and individual modules are shown with the intermediates attached to their respective ACP domains. Domains in white are proposed to be non-functional. Ibo6 is proposed to add a hydroxyl group on C16, which may induce formation of the hemiketal group and subsequent macrocyclization. Following scaffold production, the ibomycin aglycone is decorated with 7 sugars.

***Supplementary Table 1- Amino acid sequences of PKS docking domains***

<b>PKS gene</b>	<b>N-terminal docking domain</b>	<b>C-terminal docking domain</b>
<i>ibo17</i>	N/A	ALDELARLESALTASATTDERTRQE VADRLRALLRRVEPTSVDPATDPAT DAGDDDLAAASNDEIFELIDRELG
<i>ibo18</i>	EQRLRDYLN RV TADLRSTRKRLRDLEDR	Not found
<i>ibo19</i>	EERLRDYLKRASADLHRTRQKLQLETR	AEEAATWATLRTIPLRRMRETGLLD ALLALASDPTAPGGPDETAATDDT TATDQFDDMDVSDLVALALG
<i>ibo20</i>	Not found	Not found
<i>ibo21</i>	EDKLRDYLKWT TADLHETRQRLREVEEA	Not found
<i>ibo22</i>	EQKLLGYLKKVTGELRV AHRRLKEIEAA	SSELDRL EATLLALPAPEVARLRLSS RLQQLMKRLEAGADTDDSGAISAKI EAATSEDIFDLIDNEIG
<i>ibo23</i>	EDKLLEYLKKVTLELHDTKQRLRDVEAA	N/A

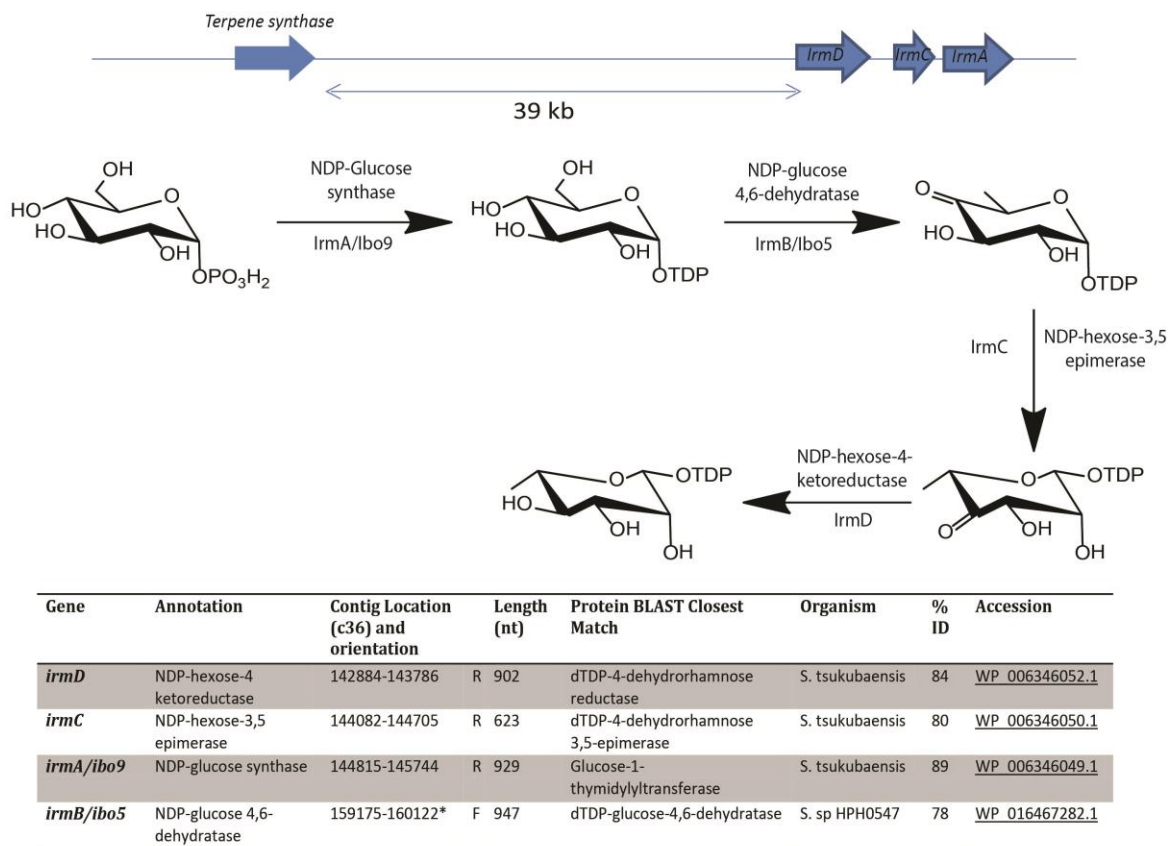
Load	VLVFPQQGA -49-VVQPA-21- VVGH <sup>S</sup> QGEI-17- VCVRS-68- AVDYASHSPAMD	MeMal
AT1	VFVFPQQG -52-VVQPA-21- VVGH <sup>S</sup> QGEI-17- VALRS-71- PVDYASHSAQVE	MeMal
AT2	VFVFPQQGA -52-VVQPA-21- VVGH <sup>S</sup> QGEI-17- VCLRS-71- PVDYASHSPQVE	MeMal
AT3	VLVFPQQGA -49-VVQPA-21- VVGH <sup>S</sup> QGEI-17- VCVRS-68- AVDYASHSPAMD	MeMal
AT4	VLVFPQQGA -49-VVQPA-21- VVGH <sup>S</sup> QGEI-17- VCVRS-68- AVDYASHSPAMD	MeMal
AT5	AFLFSGQGA -95-YTQPA-21- LIGH <sup>S</sup> VGEL-17- VATRG-67-KVSHA <sup>FH</sup> SAHMD	Mal
AT6	AFMFSGQGA -50-YTQPA-21- LIGH <sup>S</sup> VGEL-17- VAARA-65-SVSHA <sup>FH</sup> SHQMD	Mal
AT7	VFVFPQGS -52-IVQPA-21- VVGH <sup>S</sup> QGEI-17- VCLRG-70- PINYASHSAHAD	MeMal*
AT8	VLVFPQQGA -52-VVQPA-21- VVGH <sup>S</sup> QGEV-17- VVAR-67- AMDFA <sup>SH</sup> SPAME	MeMal*
AT9	GVVFSGQGG-51-WAQPA-21- LVGH <sup>S</sup> VGEL-17- VAARA-65- EVSHA <sup>FH</sup> SGLMD	Mal
AT10	VFVFPQGS -52-VVQPA-21- VGH <sup>S</sup> QGEI-17- VCLRS-70- PVTYASHCAHVD	MeMal
AT11	GVVFSGQGG-51-WAQPA-21- LVGH <sup>S</sup> VGEL-17- VAARA-65- EVSHA <sup>FH</sup> SGLMD	Mal
AT12	GVVFSGQGG-51-WAQPA-21- LVGH <sup>S</sup> VGEL-17- VAARA-65- EVSHA <sup>FH</sup> SGLMD	Mal
AT13	VLVFPQQGA -49-VVQPA-21- VVGH <sup>S</sup> QGEI-17- VCVRS-68- AVDYASHSPAMD	MeMal*
AT14	GVVFSGQGG-51-WAQPA-21- LVGH <sup>S</sup> VGEL-17- VAARA-65- EVSHA <sup>FH</sup> SGLMD	Mal*
AT15	AMVFSGQGG-51-WAQPA-21- LVGH <sup>S</sup> VGEL-17- VAARA-65- EVSHA <sup>FH</sup> SGLMD	Mal
AT16	GVVFSGQGG-51-WAQPA-21- LVGH <sup>S</sup> VGEL-17- VAARA-65- EVSHA <sup>FH</sup> SGLMD	Mal
AT17	GVVFSGQGG-51-WAQPA-21- LVGH <sup>S</sup> VGEL-17- VAARA-65- EVSHA <sup>FH</sup> SGLMD	Mal
AT18	GVVFSGQGG-51-WAQPA-21- LVGH <sup>S</sup> VGEL-17- VAARA-65- EVSHA <sup>FH</sup> SGLMD	Mal
AT19	AFLFTQGS -59-HAQPA-21- LVGH <sup>S</sup> VGEL-17- VAARG-65-RVSHA <sup>FH</sup> SARME	Mal

**Supplementary Figure 2: Sequence alignment of AT domains.** Conserved active site residues are in red and the catalytic serine is highlighted in green. Boxed sequences are those that dictate substrate specificity, in particular the highlighted residues (blue for methylmalonate and yellow for malonate). Asterisks indicate where there is a difference in the predicted substrate and what is actually seen in the structure of ibomycin. These discrepancies are seen in AT7, AT8, AT13 and AT14.



Gene	Annotation	Contig Location (c14) and orientation	Length (nt)	Protein BLAST Closest Match	Organism	% ID	Accession
<i>ivaC</i>	C3 methyltransferase	4400-5626 F	1226	Putative C-3 methyltransferase	<i>A. orientalis</i>	70	<a href="#">CCD33145.1</a>
<i>ivaB</i>	C3 transaminase	10082-11191 F	1109	Daunorubicin biosynthesis sensory transduction protein Dnj	<i>Nocardiopsis xinjiangensis</i>	75	<a href="#">WP_017609335.1</a>
<i>ivaD</i>	C3,5 epimerase	11521-12213 F	692	Putative 3,5 epimerase	<i>A. balhimycina</i> DSM 5908	60	<a href="#">WP_020646231.1</a>
<i>ivaE</i>	C4 ketoreductase	12206-13225 F	1019	NDP-4-keto-6-deoxyhexose 4 ketoreductase	<i>S. venezuelae</i> ATCC 10712	52	<a href="#">AAL14256.1</a>
<i>ivaA</i>	C2 dehydratase	87692-89071 F	1379	NDP-hexose 2,3-dehydratase	<i>S. cyanogenus</i>	70%	<a href="#">AAD13549.1</a>

**Supplementary Figure 3: Vancosamine biosynthesis genes.** Genes involved in the synthesis of vancosamine were found on contig 14 and annotated as *ivaA-E*. A schematic for the role of each enzyme in the pathway is shown. Although all genes were found on the same cluster, *ivaA* was found 74 kb downstream of the others, embedded within a biosynthetic cluster for an NRPS-PKS hybrid molecule.

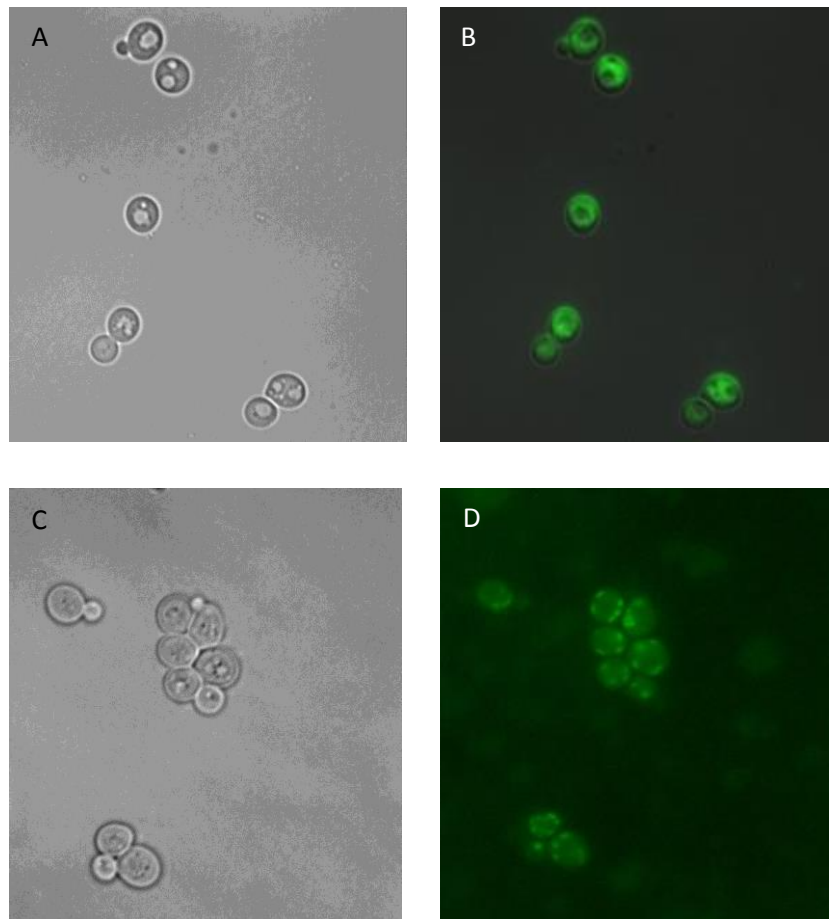


\*Located on c54 with ibomycin cluster

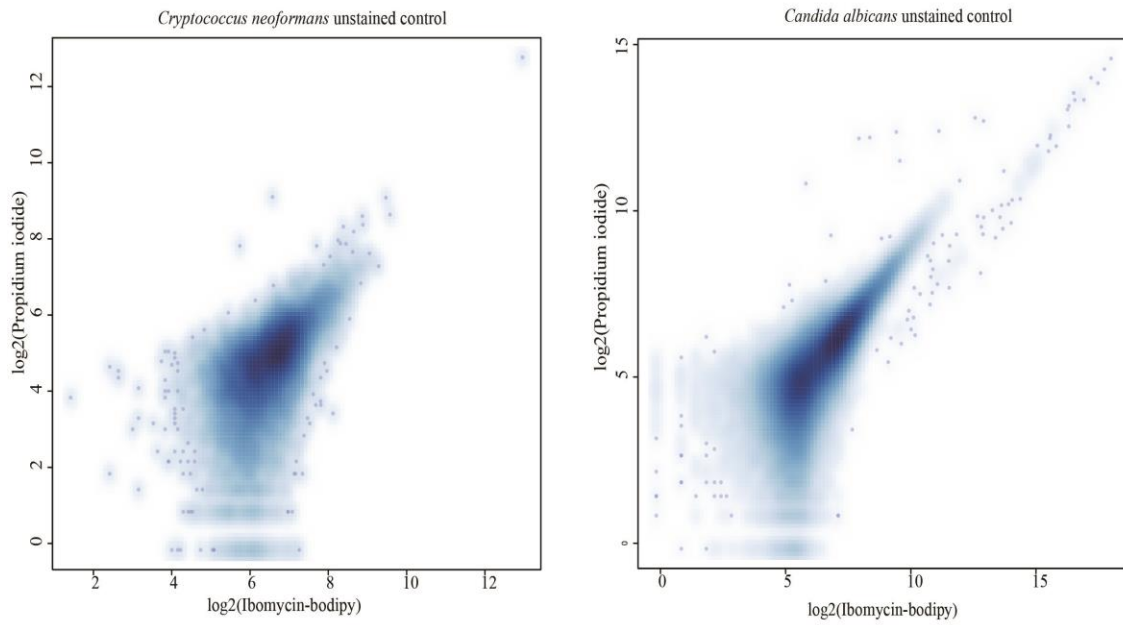
**Supplementary Figure 4: Rhamnose biosynthesis genes.** Genes involved in the synthesis of rhamnose are found on contig 36 (downstream of a predicted terpene biosynthesis cluster) and have been annotated as *irmA-D*, with the exception of *irmB* whose function overlaps with that of *ibo5*. Similarly an alternative for *irmA* is *ibo9* which is also involved in rhodinosin biosynthesis. A schematic for the role of each enzyme in the pathway is shown.

**Supplementary Table 2-Primer sequences for amplification of upstream bar-coded tags from *S. cerevisiae* deletion strains**

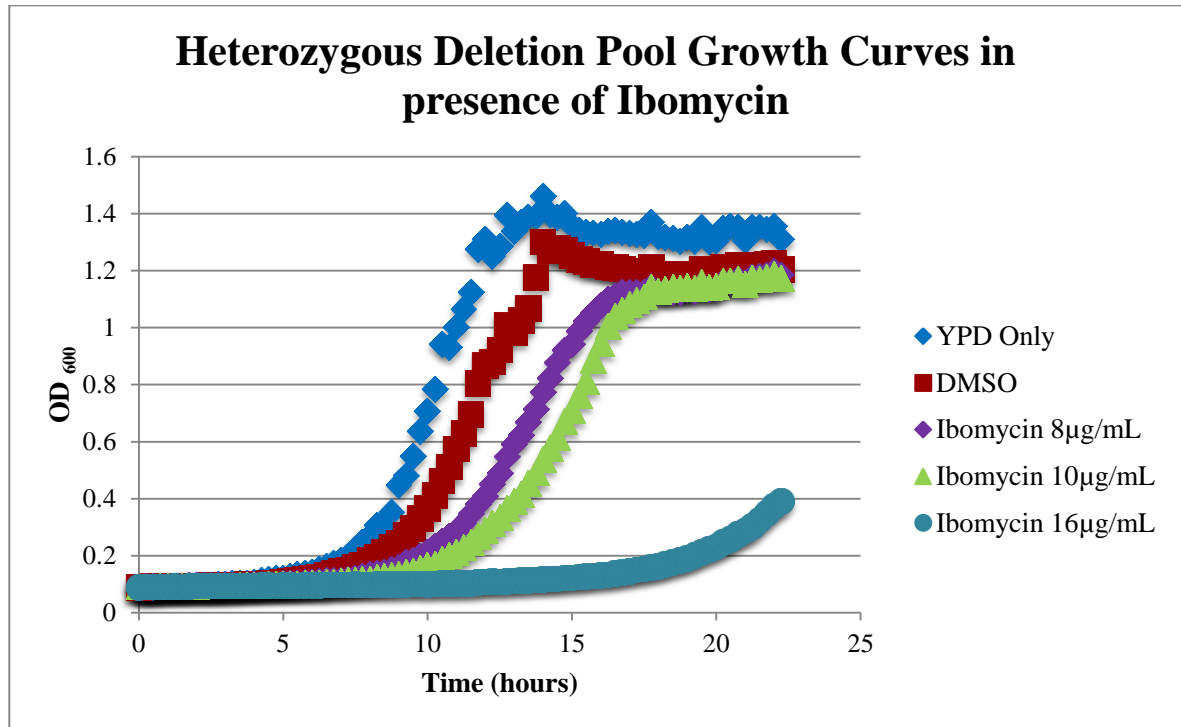
<b>Experiment</b>	<b>Forward Primer</b>	<b>Reverse Primer</b>
HIP-DMSO	AATGATACGGCGACCACCGAGATCT ACACTAGATCGCACACTCTTTCCCTA CACGACGCTCTTCCGATCTGATGTCC ACGAGGTCTCT	CAAGCAGAAGACGGCATAACGAG ATCATGCCTAGTGACTGGAGTTC AGACGTGTGCTCTTCCGATCTCCT TGACAGTCTTGACGTGC
HIP-8 µg/mL ibomycin	AATGATACGGCGACCACCGAGATCT ACACCTCTCTATACTCTTTCCCTA CACGACGCTCTTCCGATCTGATGTCC ACGAGGTCTCT	CAAGCAGAAGACGGCATAACGAG ATCATGCCTAGTGACTGGAGTTC AGACGTGTGCTCTTCCGATCTCCT TGACAGTCTTGACGTGC
HIP-10 µg/mL ibomycin	AATGATACGGCGACCACCGAGATCT ACACTATCCTCTACTCTTTCCCTA CACGACGCTCTTCCGATCTGATGTCC ACGAGGTCTCT	CAAGCAGAAGACGGCATAACGAG ATCATGCCTAGTGACTGGAGTTC AGACGTGTGCTCTTCCGATCTCCT TGACAGTCTTGACGTGC
HOP-DMSO	AATGATACGGCGACCACCGAGATCT ACACAGAGTAGAACACTCTTTCCCTA CACGACGCTCTTCCGATCTGATGTCC ACGAGGTCTCT	CAAGCAGAAGACGGCATAACGAG ATCATGCCTAGTGACTGGAGTTC AGACGTGTGCTCTTCCGATCTCCT TGACAGTCTTGACGTGC
HOP-8 µg/mL ibomycin	AATGATACGGCGACCACCGAGATCT ACACCTCTCTATACTCTTTCCCTA CACGACGCTCTTCCGATCTGATGTCC ACGAGGTCTCT	CAAGCAGAAGACGGCATAACGAG ATTTCGCTTAGTGACTGGAGTTCA GACGTGTGCTCTTCCGATCTCCTT GACAGTCTTGACGTGC
HOP-10 µg/mL ibomycin	AATGATACGGCGACCACCGAGATCT ACACAGAGTAGAACACTCTTTCCCTA CACGACGCTCTTCCGATCTGATGTCC ACGAGGTCTCT	CAAGCAGAAGACGGCATAACGAG ATTTCGCTTAGTGACTGGAGTTCA GACGTGTGCTCTTCCGATCTCCTT GACAGTCTTGACGTGC



**Supplementary Figure 5: Differential staining between bodipy and ibomycin-bodipy.** Panels (A) and (B) show the brightfield and overlay images respectively, of *S. cerevisiae* cells stained with Bodipy-FL C<sub>5</sub>. Panels (C) and (D) show the brightfield and overlay images respectively of *S. cerevisiae* cells stained with ibomycin-bodipy. Along the fluorescent probe bodipy-FL C<sub>5</sub> stains the entire cell. In contrast, the ibomycin-bodipy conjugate can be seen as small punctae on the periphery of cells, suggesting membrane localization.



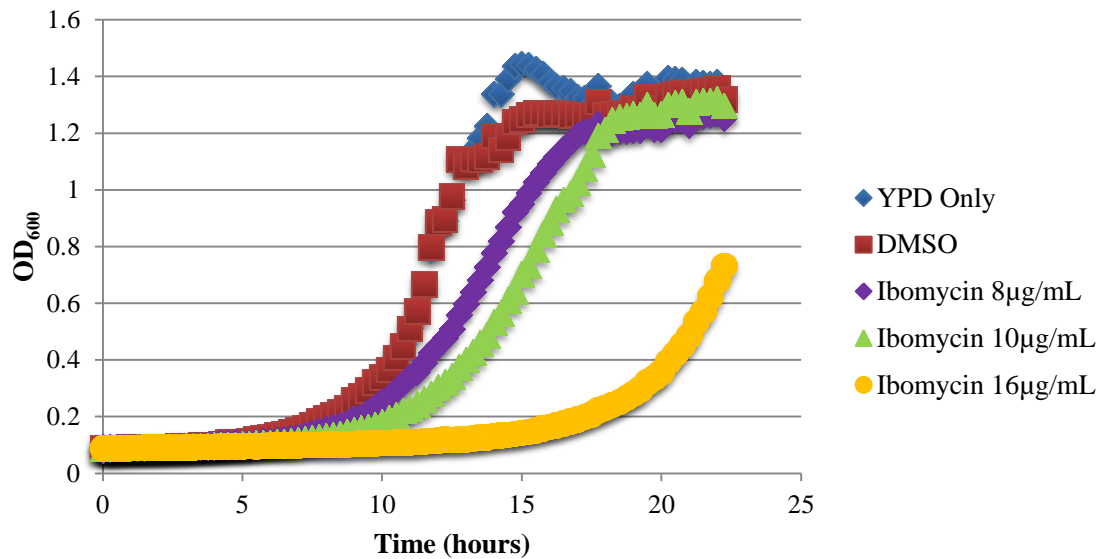
**Supplementary Figure 6: Unstained control samples of *C. neoformans* and *C. albicans*.** The plots above show the background fluorescence for ibomycin-bodipy and propidium iodide in unstained samples of the yeasts. Axes are set on a logarithmic scale. Areas that are dark blue indicate high density of cells.



***Supplementary Figure 7: Growth curves of heterozygous deletion pool mutants in presence of ibomycin.***

Based on the growth curves, genomic DNA for bar-code sequencing was harvested from cultures treated with 8 and 10 µg/mL of ibomycin as they showed a 10-30% reduction in growth compared to the solvent control. Sequencing results revealed that bar-code counts for both samples were approximately similar and thus the results from the HIP reaction with 10 µg/mL ibomycin was used for data analysis.

## Haploid Deletion Pool Growth curves in presence of ibomycin



**Supplementary Figure 8: Growth curves of haploid deletion pool mutants in presence of ibomycin.** Based on the growth curves, genomic DNA for bar-code sequencing was harvested from cultures treated with 8 and 10 µg/mL of ibomycin as they showed a 10-30% reduction in growth compared to the solvent control. Sequencing results from the HOP reaction with 10 µg/mL of ibomycin did not yield enough counts for a majority of tags and thus was not used for further data analysis.

**Supplementary Table 3- P-values for HIP hits grouped by GO processes**

<b>GO Process</b>	<b>P (0.05) value</b>
chromatin modification	8.26E-09
regulation of transcription, DNA-dependent	4.47E-04
transcription, DNA-dependent	2.953E-03
protein transport	1.5297E-02
nucleosome disassembly	3.07E-07
transcription elongation from RNA polymerase II promoter	6.73E-06
mitochondrion inheritance	2.17E-06
histone acetylation	1.75E-05
ATP-dependent chromatin remodeling	2.87E-05
RNA polymerase II transcriptional pre-initiation complex assembly	1.74E-04
transcription from RNA polymerase II promoter	4.532E-03
phospholipid transport	0
Arp2/3 complex-mediated actin nucleation	8.14E-06
nucleosome mobilization	8.14E-06
chromatin organization	7.92E-05
regulation of actin filament polymerization	7.92E-05
transcription initiation, DNA-dependent	0.000156
chromatin remodeling	0.001583
cytokinesis	0.002029
protein folding	0.008455
positive regulation of transcription from RNA pol II promoter	0.022812
vesicle-mediated transport	0.048416

**Supplementary Table 4- P-values for HOP hits grouped by GO Processes**

<b>GO Process</b>	<b>P (0.05) value</b>
transport	4.08E-05
protein transport	2.30E-07
endocytosis	1.40E-09
protein targeting to vacuole	1.88E-10
ubiquitin-dependent protein catabolic process via the MVS pathway	1.62E-12
intracellular protein transport	2.93E-06
vesicle-mediated transport	0.000142
late endosome to vacuole transport	1.86E-09
protein retention in Golgi apparatus	9.46E-10
Golgi to vacuole transport	1.52E-07
chromatin modification	0.002039
response to stress	0.016648
intraluminal vesicle formation	1.99E-09
GPI anchor biosynthetic process	8.41E-07
actin cortical patch localization	2.27E-06
actin cytoskeleton organization	5.14E-05
fungus-type cell wall organization	0.010474
carbohydrate metabolic process	0.018553
protein targeting to membrane	2.16E-05
vacuole fusion, non-autophagic	0.000281
response to osmotic stress	0.000526
actin filament organization	0.001051
chromatin remodeling	0.002707
protein glycosylation	0.00419
pseudohyphal growth	0.00934
mRNA processing	0.038788
lipid tube assembly	0
protein retention in ER lumen	2.46E-05
negative regulation of transcription from RNA polymerase II promoter by glucose	0.00012
phospholipid translocation	0.000326
negative regulation of translation	0.000483
maintenance of cell polarity	0.000483
histone exchange	0.000483
actin cortical patch assembly	0.000681
vesicle fusion	0.000681
sphingolipid biosynthetic process	0.000924

cell communication	0.001215
vacuole inheritance	0.001558
bipolar cellular bud site selection	0.001558
intracellular mRNA localization	0.001558
mRNA 3--end processing	0.001558
retrograde transport, endosome to Golgi	0.001957
chronological cell aging	0.002931
lipid transport	0.004157
exocytosis	0.010671
transcription elongation from RNA polymerase II promoter	0.013214
piecemeal microautophagy of nucleus	0.013214
ER-associated protein catabolic process	0.020966
invasive growth in response to glucose limitation	0.030741
small GTPase mediated signal transduction	0.030741
chromatin silencing at telomere	0.037573